universität wien

MASTERARBEIT / MASTER'S THESIS

Titel der Masterarbeit / Title of the Master's Thesis

„SModelS: A new physics tool - Development towards signatures beyond missing energy“

verfasst von / submitted by

Alicia Wongel BSc

angestrebter akademischer Grad / in partial fulfilment of the requirements for the degree of

Master of Science (MSc)

Wien, 2019 / Vienna, 2019

Studienkennzahl lt. Studienblatt / degree programme code as it appears on the student record sheet:	A 066 876
Studienrichtung lt. Studienblatt / degree programme as it appears on the student record sheet:	Masterstudium Physik UG2002
Betreut von / Supervisor:	Dipl.-Ing. Dr. Wolfgang Waltenberger, Privatdoz.
Mitbetreut von / Co-Supervisor:	

Abstract

`SModelS` is a tool designed to decompose Beyond the Standard Model (BSM) theories with a Z_2-symmetry and confront them with results from the LHC experiments at CERN. The code uses simplified model results to achieve the task in a model independent way. The existing version focuses on searches for supersymmetry with missing energy (MET) final states and includes a large variety of searches from the experiments ATLAS and CMS. Ongoing development is aimed at exploring beyond MET signatures of current interest within the theory and experimental communities. A first step in this direction was taken in the last release where results with heavy stable charged particles were included for the first time.

The upcoming `SModelS` update is presented which includes a completely object oriented description of the particles and thus allows to probe BSM models containing non-MET signatures more generally. The modifications facilitate the inclusion of the particles' properties such as mass and lifetime which is imperative to investigate other signatures. Results with a lifetime dependence can now be handled and an example thereof is shown.

Zusammenfassung

Die Software `SModelS` zerlegt Theorien jenseits des Standardmodells, die eine Z_2-Symmetrie aufweisen und konfrontiert diese mit Ergebnissen des LHC Experiments am CERN. Es werden Ergebnisse in Form von vereinfachten Modellen verwendet, wodurch der Vergleich modellunabhängig durchgeführt werden kann. Die aktuelle Version ist fokussiert auf Ergebnisse mit fehlender Energie (MET) im Endzustand und enthält derzeit über 100 solcher Ergebnisse von den Experimenten ATLAS und CMS. Da sowohl in der Theorie als auch bei den Experimenten das Interesse an Suchen mit anderen Endzuständen als fehlender Energie stetig wächst, wird `SModelS` derart weiterentwickelt. Ein erster Schritt in dieser Richtung wurde in der letzten Veröffentlichung getan, in der einige Ergebnisse mit schweren stabilen geladenen Teilchen im Endzustand hinzugefügt wurden.

In dieser Arbeit wird die neuste Version von `SModelS` präsentiert, die demnächst veröffentlicht wird. Diese beinhaltet die Einführung einer komplett objekt-orientierten Beschreibung der Teilchen, wodurch ermöglicht wird, dass Ergebnisse mit anderen Endzuständen als fehlender Energie auf eine generelle Art und Weise untersucht werden können. Die Modifizierung vereinfacht es, die Eigenschaften der Teilchen wie Masse und Eigenzeit zu handhaben, was für solche Ergebnisse notwendig ist. Es wird gezeigt, wie nun auch Ergebnisse, die eine Abhängigkeit von der Halbwertszeit der Teilchen aufweisen, verwendet werden können und ein Beispiel dafür wird präsentiert.

Contents

1 Introduction **6**

2 The Standard Model of particle physics **8**
2.1 The particles of the Standard Model 8
2.2 The interactions of the Standard Model 9
2.2.1 The QED sector 9
2.2.2 The QCD sector 11
2.2.3 The electroweak sector 13
2.2.4 The Higgs sector 15
2.3 Indications for physics beyond the Standard Model 17

3 Supersymmetry **22**
3.1 Particles in the Minimal Supersymmetric Standard Model (MSSM) 22
3.2 Supersymmetry breaking 24
3.3 Mixing of gauginos and higgsinos 24
3.4 R-parity 24
3.5 Searches for sparticles at the LHC 25

4 Long-lived particles **26**
4.1 Theoretical motivation 26
4.2 Detector signatures of long-lived particles 27
4.2.1 A general collider detector 28
4.2.2 Anomalous Ionization 29
4.2.3 Delayed signals 29
4.2.4 Disappearing Tracks 30
4.2.5 Displaced Tracks and Displaced Vertices (DV) 30
4.2.6 Displaced Calorimeter Deposits 31

5 The `SModelS` framework **32**
5.1 Simplified Model Spectra 32
5.2 Basic principles of `SModelS` 33
5.2.1 Parameter file 34
5.2.2 Terminology 34
5.2.3 Theory input 35
5.2.4 Experimental database 37
5.2.5 Confronting theory predictions with experimental limits 38
5.2.6 The `SModelS` output 38
5.2.7 Missing topologies 39
5.3 `SModelS` version 1.2 39
5.3.1 Decomposition 40
5.3.2 Final states 40
5.3.3 Inclusive results 40
5.3.4 Reweighting 41
5.3.5 Displaced signatures in missing topologies 41

6 `SModelS` version 2.0 - New implementations **43**
6.1 Particle class 43
6.2 Reading the input file 44
6.3 Decomposition 44

6.4 MultiParticle 45
6.5 Particle types 45
6.6 Element comparison 46
6.7 Combining elements 47
6.8 Element compression 48
6.9 Element clustering 48
6.10 Missing topologies 49
6.11 Validation 49

7 Lifetime dependent results **50**
7.1 Impact of finite lifetimes on the cross section 50
7.2 Reweighting in `SModelS` version 1.2 52
7.3 Reweighting in `SModelS` version 2.0 54
7.3.1 Dependence on the kinematic factor 54
7.3.2 Reweighting MET results and missing topologies 55
7.3.3 Calculating lifetime dependent result maps 56
7.3.4 Visualization of the lifetime reweighting 57
7.3.5 Interpolation 58

8 Summary and Outlook **59**

1 Introduction

The Standard Model (SM) of particle physics is the most successful theory to describe the world on microscopic scales. It covers all fundamental forces of nature but gravity and defines the elementary particles and their interactions. Its predictions have been confirmed to very high precision and the detection of the Higgs boson in 2012 [1, 2] completed the observation of all particles in the Standard Model. Even though the measurements of many processes are in very good agreement with the predictions of the SM, there are some observations that cannot be explained by it. Dark matter, which describes the gravitational effects observed for instance in galaxies that cannot be accounted for by visible matter and the matter-antimatter asymmetry which cannot be generated by any mechanism in the Standard Model are two examples.

Because of these limitations of the SM it is expected that there exists a more fundamental theory which explains all or parts of the observations and is not yet understood. Many extensions have been developed that include the Standard Model with its predictions as well as theoretical descriptions for the phenomena that are not explained by the SM. As these models extend the SM they are typically referred to as physics Beyond the Standard Model (BSM) and oftentimes predict new particles. The number of such theories grows constantly while at the same time ever tighter limits on the predictions made by these theories are set by the experiments. Experimental searches investigate certain parameters of specific models like the masses of the new particles. When no particles are found at a certain mass upper limits on the cross sections of processes with particles of that mass are set. The experiments setting the strongest limits on new theories in the high energy range are carried out at the Large Hadron Collider (LHC) which is located at the European Organization for Nuclear Research (CERN). The two major detectors at the LHC are ATLAS (A Toroidal LHC ApparatuS) and CMS (Compact Muon Solenoid). They have provided the experimental proof of the existence of the Higgs particle. It was hoped that they would also provide experimental evidence for any form of new physics but no such observations have been made up to this date. Instead, the experiments exclude ever more values of the properties like the masses of potentially new particles. To bring together the vast amounts of new theories and exclusion results from the experiments the software tool `SModelS` was developed. It tests full theory models against so-called simplified model results given by the experiments. Consequently, it can determine whether the theory has been excluded by experiments. `SModelS` does this in a fast and model independent way. The `SModelS` database of experimental results which is used to constrain the input theories consists of ATLAS and CMS simplified model results. `SModelS` is therefore limited by the applicability of the database results to new theories.

When the LHC was built it was thought that the most likely cases of new physics would be realized in terms of particles that are noticeably more massive than the SM particles and are very unstable. Such particles would decay right after they have been produced. Due to certain conservation rules a likely scenario for these particles was expected to be that they would cascade decay into SM particles and the lightest charge and color neutral new particle. These lightest neutral new particles would not leave a signature in the detector but could only be determined by applying the principle of energy-momentum conservation. They could then be indirectly identified as missing energy that can not be accounted for by any other known particle. Being so heavy that high energies are required to produce the BSM particles and only appearing in form of missing energy were thought to be among the reasons why they have not been seen. However, even after the LHC has been run successfully for several years no such signs of new particles have been seen in searches for missing energy.

Accordingly, there is a growing interest in searches for more exotic signatures other than missing energy, both in the theory and the experimental communities. One interesting group of these signatures is comprised of the long-lived particles. These are charge or color non-neutral new particles that live for a sufficiently long time to travel macroscopic distances before decaying.

They would therefore leave characteristic signatures in the detectors such as charged tracks with large differential energy loss. As the particle's lifetime is a critical parameter in these searches their results are oftentimes presented with a lifetime dependence which is not the case for missing energy searches.

As `SModelS` is continuously being extended with new results from ATLAS and CMS, searches for long-lived particles also need to be introduced. To also include searches looking for long-lived particles in the `SModelS` database of experimental results several modifications of its functionality are necessary. Especially the lifetime dependence of the results necessitates alterations as all previously introduced results in `SModelS` were missing energy searches without this property. The extension and restructuring of the tool is presented in this thesis as well as the introduction of lifetime dependent results of searches for long-lived particles to the database.

This thesis is organized as follows. In section 2 the main aspects of the Standard Model will be presented. Its shortcomings in describing observations will be described which motivate the searches for physics beyond the Standard Model. One example for such new physics will be given in section 3 where the basic principles of supersymmetry are outlined. Theoretical motivations for long-lived particles and the expected detector signatures associated with them are explained in section 4. In section 5 the software tool `SModelS` is presented and its major modifications necessary to handle long-lived particles are described in section 6. Details on the lifetime dependent results that can now be used in the tool and how the lifetime dependence is dealt with for the results that do not have this property is outlined in section 7. The thesis is concluded by a summary of the work that has been carried out and a description of the steps still necessary to finalize this upcoming update of `SModelS`.

2 The Standard Model of particle physics

The SM is the most accurate description of the fundamental microscopic interactions that we have today. It is in astonishing agreement with experimental findings and predicts most phenomena in elementary particle physics accurately. It describes three of the four fundamental forces of nature: the electromagnetic force that binds electrons to the nucleon, the strong force that holds protons and neutrons together in the nucleon and the weak force explaining the nuclear reactions in stars. The fourth fundamental force is gravity which is not included in the SM because it has not been possible to quantize general relativity yet. Even though gravity determines many processes of everyday life, it can safely be neglected when considering processes of fundamental particles. Because of the tiny masses of the elementary particles the gravitational force acting on them is simply extremely weak.

Furthermore, phenomena like dark matter or matter-antimatter asymmetry have been observed that cannot be explained by the SM. Therefore, it is assumed that the SM has to be extended to be able to explain these effects which is commonly referred to as new physics or physics Beyond the Standard Model (BSM). This motivates theoretical particle physicists to develop new models that are capable of describing the known particles as well as new ones which account for the yet unexplained effects. Experiments at large colliders like the LHC at CERN search for the new particles but are limited by the available energy. A brief summary of the Standard Model and its shortcomings will be given in this section. Among many others, excellent elaborations can be found in [3], [4] and [5].

2.1 The particles of the Standard Model

The SM is a Quantum Field Theory (QFT), it combines classical field theory with quantum mechanics and special relativity. It describes the electromagnetic, weak and strong interactions. The forces are mediated by the spin-1 gauge fields called gauge bosons. The spin-$\frac{1}{2}$ matter fields are called fermions.

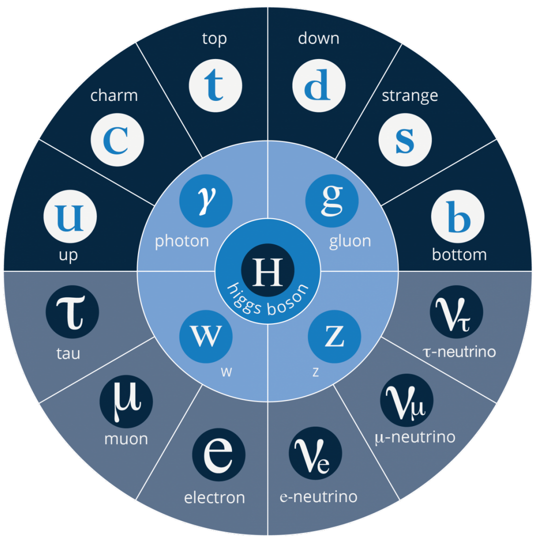

Figure 1: Particle content of the Standard model, the scalar Higgs boson is in the center surrounded by the four vector bosons. The fermions are displayed on the outer ring where the quarks are shown in the upper half and the leptons in the lower half. Figure taken from [6].

There is one neutral gauge boson, the photon, for the electromagnetic force. There are 3 gauge bosons for the weak force. Two are charged, the $W^{\pm}$-bosons and one is neutral, the Z^0-boson. For the strong force, there are 8 neutral gauge bosons, the gluons. The photon and the gluons are massless because the associated charges, the electric and the color charge, which are the symmetry generators are exactly conserved. For the weak force this is not the case, the symmetry is broken by the Higgs mechanism (outlined below) and so the weak gauge bosons are massive. The scalar and neutral Higgs boson is a consequence of the Higgs mechanism. It was the last particle of the Standard Model to be discovered experimentally in 2012.

The fermions make up all visible matter and are split into color neutral leptons and color charged quarks. They consist of three generations, however it is not known at present time why there are exactly three. The three generations have identical quantum numbers but different masses. The fermions can be arranged in left-handed doublets and right-handed singlets with increasing mass from left to right as shown in Tab.1. The handedness refers to the chirality of the particle. Chirality describes the relation of the spin of a particle and its direction of propagation and will be further discussed in section 2.2.3.

	1st gen.	2nd gen.	3rd gen.
leptons:	$\binom{\nu_e}{e^-}_L \; e^-_R$	$\binom{\nu_\mu}{\mu^-}_L \; \mu^-_R$	$\binom{\nu_\tau}{\tau^-}_L \; \tau^-_R$
quarks:	$\binom{u}{d} \; u_R, d_R$	$\binom{s}{c} \; s_R, c_r$	$\binom{t}{b} \; t_R, b_R$

Table 1: Fermions in the Standard model and their properties

Each lepton generation consists of a doublet of a neutrino and an electrically charged lepton. The lightest charged lepton is the electron with a mass of 0.5 MeV [7] and the heaviest is the tau with a mass of 1777 MeV [7]. The neutrinos are massless in the SM but it was shown experimentally that they do have very small masses (see section 2.3). The quarks form doublets of an up-type and a down-type quark with each quark appearing in three different colors. Additionally, for every fermion there exists an antiparticle with opposite electric and color charge. Neutrinos are charge and color neutral and only differ from their antiparticle in chirality. It remains an open question whether the neutrino is its own antiparticle as they only differ in helicity while all other quantum numbers are the same.

2.2 The interactions of the Standard Model

After introducing the particles of the SM, the different sectors of the SM and their interactions will now be discussed separately. The local gauge group of the SM is $\mathrm{U(1)_Y \times SU(2)_L \times SU(3)_C}$, corresponding to the electromagnetic, weak and strong force. The indices represent the corresponding charges which are the generators of the respective symmetry group. Here, Y stands for the hypercharge, L stands for left-handedness and C stands for color charge. Further details will be given in the dedicated sections. Natural units where $\hbar = c = 1$, with $\hbar$ being the reduced Planck constant and c the speed of light, are applied throughout the entire thesis unless stated otherwise.

2.2.1 The QED sector

Quantum electrodynamics (QED) is considered the best theory ever built to describe nature at short distances because it could be verified experimentally to the highest precision ever achieved by mankind. The most astonishing agreement between theory and experiment comes from calculations and measurements of the anomalous magnetic moments a of the electron and muon. They are defined as

$$a = \frac{g-2}{2}. \tag{1}$$

g is the gyromagnetic ratio which relates the magnetic moment $\vec{\mu}$ of a particle to its spin $\vec{S}$ according to

$$\vec{\mu} = g\frac{e}{2m}\vec{S} \tag{2}$$

where m is the mass of the particle and e is the electric unit charge. The anomalous magnetic moments result from virtual electrons and photons. These contributions can be computed in terms of the QED fine structure constant $\alpha = \frac{e^2}{4\pi}$ according to

$$a = \frac{g-2}{2} = C_1\frac{\alpha}{\pi} + C_2\left(\frac{\alpha}{2\pi}\right)^2 + C_3\left(\frac{\alpha}{2\pi}\right)^3 + C_4\left(\frac{\alpha}{2\pi}\right)^4 + ... \tag{3}$$

where the C_i are constants. Corrections of $\mathcal{O}(\alpha^4)$ have been fully calculated giving a very precise theoretical prediction which is in line with the experimentally measured values. In turn, this also determines the fine structure constant to high accuracy as [8]:

$$\alpha^{-1} = 137.035999084 \pm 0.000000051. \tag{4}$$

Because of QED's outstanding role, the derivation of its Lagrangian will be outlined in detail. To obtain the QED Lagrangian one needs to start out with the Dirac Lagrangian describing a fermion

$$\mathcal{L}_0 = i\overline{\psi}(x)\gamma^\mu\partial_\mu\psi(x) - m\overline{\psi}(x)\psi(x) \tag{5}$$

where $\psi(x)$ is a Dirac spinor describing the fermion and $\overline{\psi}(x) = \psi(x)^\dagger\gamma^0$, m is the mass of the fermion and $\partial_\mu = \frac{\partial}{\partial\mu}$. γ^μ are the Dirac matrices defined as

$$\gamma^0 = \begin{pmatrix} 0 & 1 \\ 1 & 0 \end{pmatrix}, \gamma^i = \begin{pmatrix} 0 & \sigma^i \\ -\sigma^i & 0 \end{pmatrix} \tag{6}$$

where the σ^i are the Pauli matrices.

The Dirac Lagrangian is invariant under a global U(1) transformation

$$\psi(x) \xrightarrow{U(1)} \quad \psi'(x) \equiv \exp\{iQ\theta\}\psi(x) \tag{7}$$

with $Q\theta$ being an arbitrary constant and thus $exp(iQ\theta)$ being a convention dependent phase factor.

However, it is not invariant under a local U(1) transformation where $\theta = \theta(x)$ varies with the location as $\partial_\mu\psi(x)$ transforms like

$$\partial_\mu\psi(x) \xrightarrow{U(1)} \exp\{iQ\theta\}\left(\partial_\mu + iQ\partial_\mu\theta\right)\psi(x). \tag{8}$$

Such an invariance is however required since the global phase factor $exp(iQ\theta)$ should not depend on the choice of x. To obtain also local invariance one makes use of the gauge principle by introducing a new field A_μ, defined as

$$A_\mu(x) \xrightarrow{U(1)} A'_\mu(x) \equiv A_\mu(x) - \frac{1}{e}\partial_\mu\theta \tag{9}$$

which exactly cancels the additional term in Eq.8. One can also define a covariant derivative with the field for concise notation as

$$D_\mu\psi(x) \equiv \left[\partial_\mu + ieQA_\mu(x)\right]\psi(x) \tag{10}$$

which replaces the ordinary derivative in the Lagrangian. With this addition we arrive at the Lagrangian

$$\mathcal{L} = i\overline{\psi}(x)\gamma^\mu D_\mu\psi(x) - m\overline{\psi}(x)\psi(x) = \overline{\psi}\left(i\gamma^\mu\partial_\mu - m\right)\psi - \overline{\psi}e\gamma_\mu A^\mu\psi \tag{11}$$

which then is invariant under a local U(1) transformation. Now in order to allow for propagation of the electromagnetic field A_μ an additional kinetic term

$$\mathcal{L}_{kin} = \frac{1}{4} F_{\mu\nu} F^{\mu\nu} \tag{12}$$

is necessary with the field strength tensor $F_{\mu\nu} = \partial_\mu A_\nu - \partial_\nu A_\mu$ which is also invariant under local U(1) transformation.

A mass term for the field defined as $\mathcal{L}_{mass} = \frac{1}{2} m^2 A_\mu A^\mu$ is not allowed since this would violate gauge invariance. Consequentially, the corresponding particle, the photon, is massless.

Combining Eq.11 and Eq.12 we then arrive at the QED Lagrangian:

$$\mathcal{L}_{\mathrm{QED}} = \overline{\psi} \left(i\gamma^\mu \partial_\mu - m \right) \psi - \overline{\psi} e \gamma_\mu A^\mu \psi - \frac{1}{4} F^{\mu\nu} F_{\mu\nu}. \tag{13}$$

QED describes the electromagnetic interaction which is mediated by the photon and acts on all electrically charged matter fields in the SM, i.e. the quarks and the charged leptons. The Lagrangian in Eq.11 describes the interaction between the fermion and the field A_μ which can be visualized in a Feynman diagram [9]:

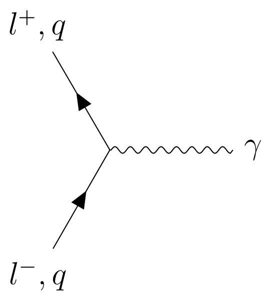

Figure 2: Feynman diagram of the fundamental QED vertex, all Feynman diagrams in this thesis are created with TikZ-Feynman [10].

in which time proceeds from left to right (as for all Feynman diagrams in this thesis). The way the diagram is oriented in Fig.2 represents electron-positron annihilation. By rotating it, one obtains a representation of pair production or emission/absorption of a photon.

2.2.2 The QCD sector

When new particles called mesons and baryons were discovered in large numbers in the second half of the 20th century the idea of them exhibiting a simpler underlying structure evolved. The mesons and baryons can be arranged in multiplets according to their quantum numbers. The quantum numbers of the mesons and baryons can be explained by assuming that they consist of more fundamental particles, the quarks. For example, the proton which has an electric charge of $+1$ consists of two up quarks with an electric charge of $+2/3$ and a down quark with an electric charge of $-1/3$. We know today that there exist six different quarks: up, down, charm, strange, top and bottom. One also refers to them as six flavors of quarks. The mesons are formed by a quark and an anti-quark while the baryons consist of three quarks. Some of the baryons were predicted and experimentally found to consist of three quarks of the same flavor like the Δ^{++}-baryon that is formed by three up-type quarks. In this case multiple identical particles would have to exist in the same state which would violate Fermi-Dirac-statistics. Therefore a new charge, the color charge was introduced. Since it neither couples to leptons nor to the carriers of the electroweak interaction it can be understood as the charge of the strong force. Color charge is the generator of the $SU(3)_C$ symmetry group. There are three color charges: red, green and blue. Observations of only color-neutral meson and baryon states are in agreement with the existence of three color charges. The confinement hypothesis predicts that no free quarks can be observed because only color neutral states are allowed.

The number of the color charges N_C can be tested experimentally by measuring the ratio of the cross sections of hadron production and muon-antimuon production in an electron-positron collider

$$R_{e^+e^-} \equiv \frac{\sigma\left(e^+e^- \rightarrow \text{ hadrons }\right)}{\sigma\left(e^+e^- \rightarrow \mu^+\mu^-\right)}. \tag{14}$$

The electroweak production factors cancel in the ratio and due to confinement all quarks hadronize. The ratio can therefore be approximated by

$$R_{e^+e^-} \approx N_C \sum_{f=1}^{N_f} Q_f^2 = \begin{cases} \frac{2}{3} N_C = 2, & (N_f = 3 : u, d, s) \\ \frac{10}{9} N_C = \frac{10}{3}, & (N_f = 4 : u, d, s, c) \\ \frac{11}{9} N_C = \frac{11}{3}, & (N_f = 5 : u, d, s, c, b) \end{cases} \tag{15}$$

where N_f is the number of quark flavors that are kinematically accessible. The experimental measurement of N_c is in very good agreement with the theoretically predicted value of 3 [7].

Applying similar arguments as for the QED Lagrangian one can derive the QCD Lagrangian. We again start with the free Lagrangian

$$\mathcal{L}_0 = \overline{\psi}_q \left(i\gamma^\mu \partial_\mu - m\right) \psi_q \tag{16}$$

where ψ_q is a quark field of color and flavor. It is invariant under transformations of the $SU(3)_C$ symmetry group

$$q_f^\alpha \longrightarrow \left(q_f^\alpha\right)' = U_\beta^\alpha q_f^\beta, \; U = \exp\left\{i\frac{\lambda^a}{2}\theta_a\right\} \tag{17}$$

where α denotes the color and f the flavor. The eight generators λ^a are the Gell-Mann-matrices which satisfy the commutation relation

$$\left[\frac{\lambda^a}{2}, \frac{\lambda^b}{2}\right] = i f^{abc} \frac{\lambda^c}{2} \tag{18}$$

with f^{abc} being the real and totally anti-symmetric structure constants. In order to satisfy that the Lagrangian again must also be invariant under local $SU(3)$ transformations we introduce 8 new fields $G_a^\mu(x)$, the gluons. A covariant derivative is defined which replaces the ordinary derivative in the Lagrangian as

$$D^\mu q_f \equiv \left[\partial^\mu + i g_s \frac{\lambda^a}{2} G_a^\mu(x)\right] q_f \tag{19}$$

which leads to a cancellation of the additional term when a local $SU(3)$ transformation is carried out. With the kinetic term allowing for the field to propagate,

$$\mathcal{L}_{kin} = -\frac{1}{4} G_a^{\mu\nu} G_{\mu\nu}^a, \tag{20}$$

where $G_{\mu\nu}$ is defined as

$$G_a^{\mu\nu}(x) = \partial^\mu G_a^\nu - \partial^\nu G_a^\mu - g_s f^{abc} G_b^\mu G_c^\nu \tag{21}$$

we then obtain the complete QCD Lagrangian:

$$\mathcal{L}_{\text{QCD}} = \overline{\psi}_q \left(i\gamma^\mu \partial_\mu - m\right) \psi_q - \overline{\psi}_q g_s \gamma_\mu \frac{\lambda_a}{2} G_a^\mu \psi_q - \frac{1}{4} G_a^{\mu\nu} G_{a\mu\nu}. \tag{22}$$

The additional kinetic term for the Lagrangian as well as the gauge transformation of the gluon fields are more complicated than in QED (note the third term in Eq.21) because of the non-commutativity of the $SU(3)_C$ matrices. Another consequence of the non-abelian commutation relation is that the strong coupling constant g_s is unique and can not be chosen arbitrarily for different fermions as was the case in QED. This means that all quark flavors couple to the gluons with the exact same coupling strength. Furthermore, the $G_{\mu\nu}G^{\mu\nu}$ term gives rise to cubic and quartic gluon self-interactions which is an entirely new feature, not present in QED. The interaction of quarks and gluon as well as the self-interactions of the gluon can again be visualized in Feynman diagrams as shown in Fig.3.

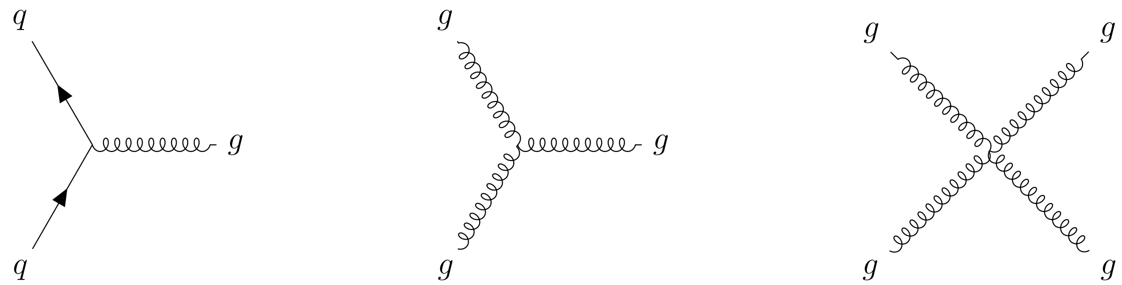

Figure 3: Feynman diagrams of the fundamental QCD vertices

2.2.3 The electroweak sector

The electroweak theory unifies the electromagnetic force and the weak force and was proposed by Weinberg, Salam and Glashow in the 1960's [11],[12],[13]. To construct a Lagrangian for the electroweak interactions once again one makes use of the principle of gauge invariance. There are, however, some additional complications compared to QED and QCD due to experimental observations regarding the weak force.

It was discovered that only fermions with left-handed chiralities and anti-fermions with right-handed chiralities take part in weak interactions. This was deduced from detailed measurements of energies and angular distributions of the particles involved in beta decay like the processes $\mu^- \rightarrow e^-\overline{\nu}_e\nu_\mu$ or $n \rightarrow pe^-\overline{\nu}_e$. The chirality of a particle is mathematically defined by its transformation behaviour under the Poincaré group. While it is not straightforward to envision this property, the closely related property helicity can be pictured more easily. The helicity of a particle is defined by the orientation of its spin vector to its direction of movement. If they are parallel, the particle has right-handed helicity and if they are anti-parallel it has left-handed helicity. For massless particles the chirality is equivalent to its helicity. For massive particles this definition is problematic because one can find a reference frame which moves faster than the particle where the direction of movement of the particle flips. So for massive particles, the helicity and chirality are distinct since the definition of helicity is not Lorentz invariant.

It was found that the photon couples to left-handed and right handed fermions in exactly the same way while the Z-boson couplings are different for fermions with different chiralities. Furthermore, the Z-boson couples only to left-handed neutrinos.

The short range of the weak interaction which was also observed in beta decay gave first hints at the large masses of the W and Z bosons which were experimentally measured to be (80.3700 ± 0.019) GeV and (91.1876 ± 0.0021) GeV [7]. The details of how the weak gauge bosons obtain there masses will be outlined in the next section.

Weak interactions are also called charged current (CC) when they are mediated by a $W^{\pm}$-boson or neutral current (NC) when being mediated by the Z-boson. Several properties of these interactions were experimentally observed. The $W^{\pm}$-boson couples to the fermion doublets of table

1, resulting in the decays

$$W^- \to e^-\overline{\nu}_e, \mu^-\overline{\nu}_\mu, \tau^-\overline{\nu}_\tau, d'\overline{u}, s'\overline{c}.$$

The decay $W^- \to b'\overline{t}$ is kinematically forbidden because of the high top mass. d', s' and b' are the mass eigenstates of the down-type quarks which are mixtures of the flavor eigenstates d, s and b. The mass and flavor eigenstates of the down-type quarks are related by

$$\begin{pmatrix} d' \\ s' \\ b' \end{pmatrix} = \mathbf{V} \begin{pmatrix} d \\ s \\ b \end{pmatrix} \tag{23}$$

where $\mathbf{V}$ is the Cabibbo-Kobayashi-Maskawa (CKM) matrix [14],[15]

$$\begin{pmatrix} d' \\ s' \\ b' \end{pmatrix} = \begin{pmatrix} V_{ud} & V_{us} & V_{ub} \\ V_{\alpha d} & V_{cs} & V_{cb} \\ V_{td} & V_{ts} & V_{tb} \end{pmatrix} \cdot \begin{pmatrix} d \\ s \\ b \end{pmatrix}. \tag{24}$$

For neutral current decays, the Z-boson decays to a pair of a fermion and its anti-fermion while conserving the flavor. This is also true for the photon, however contrary to the Z-boson it does not couple to neutrinos.

To incorporate all these properties in a Langrangian one needs a more elaborate structure than for QED or QCD. Since we need to handle both the left-handed fermion doublets and right-handed fermion singlets, the group $SU(2)_L$ is chosen, where the L stands for left-handed, which is the simplest group with doublet representations. To also include the electromagnetic interaction we need an additional $U(1)_Y$ group. This results in the symmetry group $U(1)_Y \times SU(2)_L$ for the electroweak interaction. The construction of the Lagrangian follows again the gauge principle discussed in greater detail previously. One starts from the free Lagrangian

$$\mathcal{L}_0 = i\overline{\psi}_{L/R}(x)\gamma^\mu \partial_\mu \psi_{L/R}(x) \tag{25}$$

where we differentiate between the left-handed doublets ψ_L and right-handed singlets ψ_R. It is invariant under a global $SU(2)$ transformation

$$U_L \equiv \exp\left\{ i\frac{\sigma_j}{2}\alpha^j \right\} \tag{26}$$

where the σ_i are the Pauli matrices. Requiring also local invariance results in three new fields. When requiring invariance under local $SU(2)_L \times U(1)_Y$ one therefore needs a total of four additional fields, one field B^μ from $U(1)$ and three fields W_a^μ from $SU(2)$. The Lagrangian then results in

$$\begin{aligned} \mathcal{L}_{EW} = \overline{\psi}_L i\gamma_\mu \partial^\mu \psi_L - \overline{\psi}_L \gamma_\mu \left(g\frac{\sigma_a}{2} W_a^\mu + g'\frac{Y}{2}B^\mu \right)\psi_L \\ - \overline{\psi}_R \gamma_\mu \left(g'\frac{Y}{2}B^\mu \right)\psi_R - \frac{1}{4}W_{a\mu\nu}W_a^{\mu\nu} - \frac{1}{4}B_{\mu\nu}B^{\mu\nu} \end{aligned} \tag{27}$$

where g is the electromagnetic coupling constant, g' is the weak coupling constant and Y is the hypercharge. The fields W_a^μ and B^μ can be identified with the gauge bosons $W^\pm$, Z and γ by

$$\begin{pmatrix} W_\mu^+ \\ W_\mu^- \end{pmatrix} = \frac{1}{\sqrt{2}} \begin{pmatrix} 1 & -i \\ 1 & i \end{pmatrix} \cdot \begin{pmatrix} W_\mu^1 \\ W_\mu^2 \end{pmatrix} \tag{28}$$

and

$$\begin{pmatrix} A_\mu \\ Z_\mu \end{pmatrix} = \begin{pmatrix} \cos\theta_W & \sin\theta_W \\ -\sin\theta_W & \cos\theta_W \end{pmatrix} \cdot \begin{pmatrix} B_\mu \\ W_\mu^3 \end{pmatrix} \tag{29}$$

with θ_W being the Weinberg angle defined by [16]

$$\sin^2\theta_W = 1 - \left(\frac{m_W}{m_Z}\right)^2 \approx 0.23. \tag{30}$$

In order to reobtain QED from Eq.27 one needs to identify

$$g\sin\theta_W = g'\cos\theta_W = e, \quad Y = Q - T_3 \tag{31}$$

where Y is the hypercharge, Q is the electric charge and T_3 is the weak isospin. The isospin of particle is defined in analogy to the spin. To a particle with isospin $T = \frac{1}{2}$ belong two weak isospin states $T_3 = \pm\frac{1}{2}$. Accordingly, the weak isospins are defined for the quark and leptons. The right-handed fermions have a weak isospin of zero, while the weak isospins of the left-handed quarks and leptons are defined as:

$$\begin{array}{l} T_3(u_L) = T_3(c_L) = T_3(t_L) = T_3(\nu_{l,L}) = \frac{1}{2} \\ T_3(d_L) = T_3(s_L) = T_3(b_L) = T_3(l_L) = -\frac{1}{2} \\ T_3(q_R) = T_3(l_R) = 0. \end{array} \tag{32}$$

The interactions of the weak force are summarized in Feynman diagrams in Fig.4.

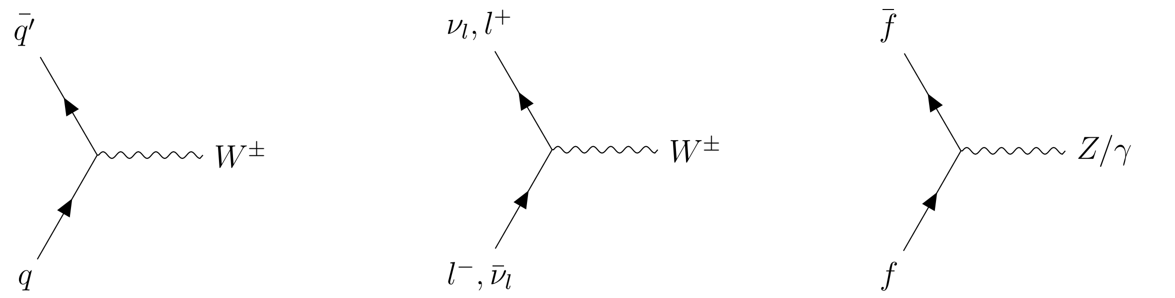

(a) Charged current interaction with q and $\bar{q}'$ being any left-handed quark doublet except for the kinematically forbidden $(t, \bar{b}')$

(b) Charged current interaction with the left-handed lepton doublets

(c) Neutral current interactions with f being any quark or lepton; the vertex with a photon interacting with two neutrinos is not allowed

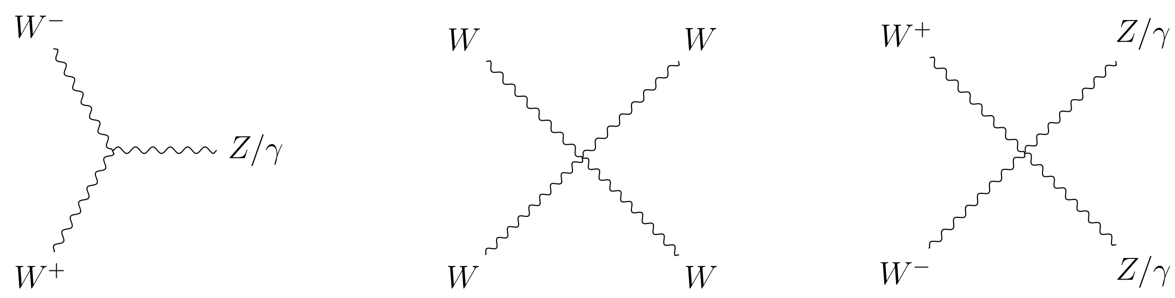

(d) Cubic self interactions of the gauge bosons

(e) Self interactions of the $W^\pm$-bosons conserving charge: $W^+W^- \to W^+W^-$ or $W^\pm W^\pm \to W^\pm W^\pm$

(f) Quartic self interactions of the gauge bosons

Figure 4: Feynman diagrams of the fundamental weak vertices

2.2.4 The Higgs sector

The Lagrangians we derived so far do not yet suffice to explain reality as the gauge bosons of the weak interaction as well as the fermions are still massless. Spontaneous symmetry breaking was proposed in the 1960's by Higgs [17], Brout and Englert [18] and gives rise to mass terms for the fermions and weak gauge bosons. The confirmation that this still leads to a renormalizable theory was given by 't Hooft several years later [19]. The idea is to build a Lagrangian that is invariant under a set of transformations and has a set of degenerate minimal energies. One introduces a complex scalar field ϕ with the Lagrangian

$$\mathcal{L} = \partial_\mu \phi^\dagger \partial^\mu \phi - V(\phi), \quad V(\phi) = \mu^2 \phi^\dagger \phi + \lambda \left(\phi^\dagger \phi\right)^2 \tag{33}$$

which is invariant under

$$\phi(x) \longrightarrow \phi'(x) \equiv \exp\{i\theta\}\phi(x). \tag{34}$$

A ground state is introduced by bounding the potential from below with $\lambda > 0$. The minimum is then dependent on μ^2. For $\mu^2 > 0$ the only minimum is given by the trivial solution $\phi = 0$. For $\mu^2 < 0$ it is given by

$$v = \langle 0|\phi|0\rangle = \sqrt{\frac{-\mu^2}{\lambda}} \tag{35}$$

and is called vacuum expectation value (VEV). It is not unique because of the $U(1)$ invariance of the Lagrangian that allows for an infinite number of possible values of $v = \sqrt{\frac{-\mu^2}{\lambda}} \exp\{i\theta\}$. By choosing a particular value for the ground state, e.g. $\theta = 0$ the symmetry then gets broken spontaneously.

A consequence of the spontaneous symmetry breaking is the existence of massless states according to the Goldstone theorem [20] which are called Goldstone bosons accordingly. It predicts that for every broken generator of a continuous global symmetry there exists a massless scalar field. After electroweak symmetry breaking we obtain three massless Goldstone bosons because there are three broken generators of the $SU(2)_L$ symmetry while the $U(1)_{QED}$ symmetry remains intact. One can then parametrize $\phi(x)$ in terms of the Higgs field as

$$\phi(x) = \exp\left\{i\frac{\sigma_j}{2}\theta^j(x)\right\} \frac{1}{\sqrt{2}} \begin{pmatrix} 0 \\ v + H(x) \end{pmatrix} \tag{36}$$

giving us in total four free fields: $\theta^i(x)$ and $H(x)$. The three fields $\theta^i(x)$ correspond exactly to the three massless Goldstone bosons. Due to the local $SU(2)_L$ invariance of the Lagrangian any dependence on $\theta^i(x)$ can be rotated away. With $\phi(x)$ from Eq.36 the kinetic term of the Lagrangian in the gauge $\theta^i(x) = 0$ in terms of the covariant derivative D_μ is then

$$\left(D_\mu \phi\right)^\dagger D^\mu \phi \quad \xrightarrow{\theta^t=0} \frac{1}{2}\partial_\mu H \partial^\mu H + (v + H)^2 \left\{\frac{g^2}{4} W_\mu^\dagger W^\mu + \frac{g^2}{8\cos^2\theta_W} Z_\mu Z^\mu\right\} \tag{37}$$

with quadratic terms for W_μ and Z^μ which are the mass terms for the $W^\pm$ and Z bosons. The mass terms for all gauge bosons can then be determined to be

$$m_h = \sqrt{2\mu^2} = \sqrt{2\lambda v^2}, \quad m_W = \frac{1}{2} g v, \quad m_Z = \frac{1}{2} v \sqrt{g^2 + g'^2}, \quad m_\gamma = 0. \tag{38}$$

One also obtains cubic and quartic terms representing the interactions among the gauge bosons.

After decades of experimental efforts the Higgs boson could finally be discovered at the LHC in 2012 and its mass measured to be (125.09 ± 0.24) GeV [7]. With the masses of the gauge bosons it now only remains to account for the masses of the fermions. One cannot introduce a term $\mathcal{L}_m = -m\overline{\psi}\psi = -m\left(\overline{\psi}_L \psi_R + \overline{\psi}_R \psi_L\right)$ because this would violate gauge symmetry. Instead, one can make use of the newly introduced scalar Higgs doublet Φ to construct a gauge invariant Lagrangian of Yukawa type

$$\mathcal{L}_Y = \sum_{\psi_d} c_{\psi_d} \left(\overline{\psi}_L \phi \psi_{d,R} + \overline{\psi}_{d,R} \phi^\dagger \psi_L\right) + \sum_{\psi_u} c_{\psi_u} \left(\overline{\psi}_L \tilde{\phi} \psi_{u,R} + \overline{\psi}_{u,R} \tilde{\phi}^\dagger \psi_L\right) \tag{39}$$

where $\tilde{\phi}$ is the conjugate field

$$\tilde{\phi} = -i\frac{\sigma_2}{2}\phi = \frac{1}{\sqrt{2}}\begin{pmatrix} v + h(x) \\ 0 \end{pmatrix}. \tag{40}$$

The constants c_i in Eq.39 define the masses and couplings of the fermions. They are arbitrary which implies that the masses of the fermions are also arbitrary. The masses can only be determined experimentally and not derived from theory.

The interactions containing a Higgs vertex are summarized in Fig.5.

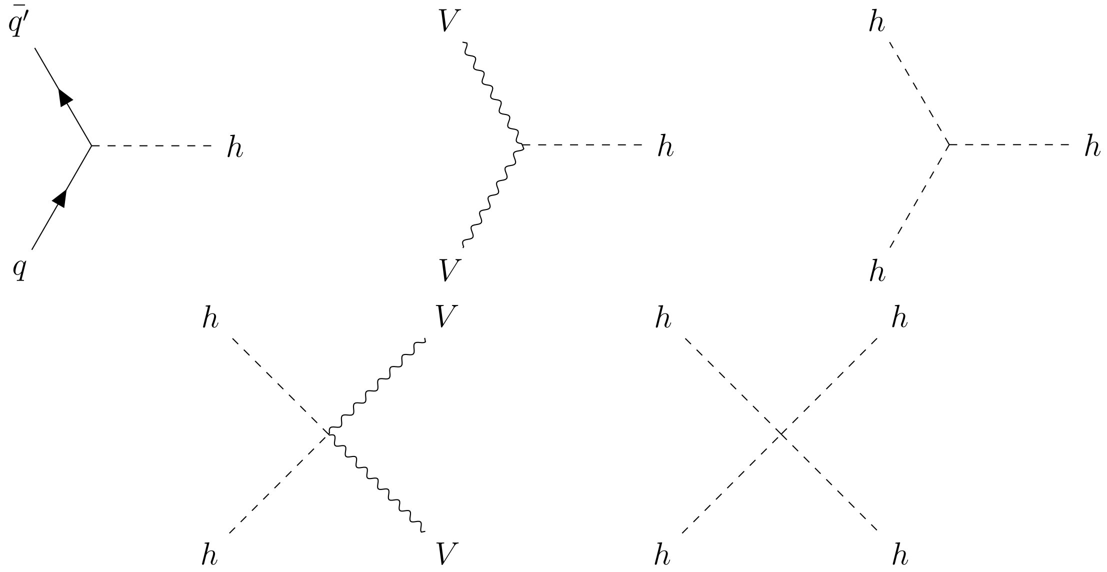

Figure 5: Feynman diagrams of the fundamental Higgs vertices. V represents a $W^{\pm}$ or a Z boson. All decays must conserve energy and be kinematically allowed.

2.3 Indications for physics beyond the Standard Model

Many predictions of the SM have been experimentally tested and confirmed with very high precision. It is so far one of the most accurate theories developed to describe matter and energy at the most fundamental scale. Nevertheless, there are some observations which cannot be explained by the SM and are interpreted as indications for new physics which we do not understand yet.

Gravity

Of the fundamental forces gravity is the only one that is not described by the Standard Model because so far it was not possible to describe gravity in terms of a quantum field theory. As stated before it is negligible at the scales we are usually concerned with when investigating particle physics. Nevertheless, it is still desirable to find a way to quantize gravity and develop a theory that is capable of explaining all forces. Physicists have tried to find a solution for many decades and it remains to be one of the most challenging open questions in the field.

Matter-antimatter asymmetry

Matter and antimatter should have been created in equal amounts in the big bang and the SM predicts the same behavior for both in most processes. Matter annihilates with antimatter, so if the same amounts of them were created with the same behavior there should have been nothing left but energy. Since this is not the case nature seems to fundamentally discriminate between matter and antimatter at a high energy scale. Behavioural differences of matter and antimatter are investigated at many high energy experiments. Examples for processes where these differences were observed are the Kaon oscillations and B meson decays. Nevertheless, the differences do not suffice to explain the matter-antimatter asymmetry observed.

Neutrino masses

In the SM Lagrangian the neutrinos are considered massless but experiments have shown that this is not the case. Observations of neutrino oscillations between the different flavors provide the strongest evidence for the neutrino masses. In the 1960's it was found that the number of observed electron neutrinos coming from the Sun does not match the number predicted from the Sun's luminosity. This observation is also known as the solar neutrino problem. The Sun is fueled by nuclear fusion according to the beta plus decay $p \rightarrow ne^+\nu_e$ releasing energy but also neutrinos. By measuring the Sun's luminosity one could then deduce the number of expected neutrinos. It was proposed that the deficiency between the numbers of experimentally observed and predicted neutrinos arises from an oscillation between the neutrino flavors. This means that the missing electron neutrinos have changed its flavor on the way to Earth and therefore could not be detected. To theoretically allow for flavor changing the particles' flavor eigenstates need to consist of combinations of the mass eigenstates analogous to the way the quark mixing works in QCD. One also receives a mixing matrix

$$\begin{pmatrix} v_e \\ v_\mu \\ v_\tau \end{pmatrix} = \begin{pmatrix} U_{e1} & U_{e2} & U_{e3} \\ U_{\mu 1} & U_{\mu 2} & U_{\mu 3} \\ U_{\tau 1} & U_{\tau 2} & U_{\tau 3} \end{pmatrix} \begin{pmatrix} v_1 \\ v_2 \\ v_3 \end{pmatrix} \tag{41}$$

which is called Pontecorvo-Maki-Nakagawa-Sakate (PMNS)-matrix [21],[22]. Experimental evidence was provided by the Super Kamiokande [23] and the SNO [24] experiments in the late 1990's and early 2000's. For both solar and atmospheric neutrinos they measured the ratios of the different flavors with high precision. Discrepancies were found between the measured values of these ratios and the values expected from the solar and atmospheric neutrino fluxes respectively. Additionally, Super Kamiokande measured a zenith angle dependence of the ratio which is considered strong evidence for neutrino oscillation as the oscillation probability depends on the distance travelled by the neutrino. For a detector close to the surface of the earth the distance travelled by the neutrino differs significantly depending on the direction where it is coming from. For example, an atmospheric neutrino travelling vertically downward travels a much shorter distance as opposed to one travelling vertically upward which also has to travel through the Earth. As the exact nature of the neutrinos is unknown, one can either consider them to be Dirac like the SM leptons or Majorana, making them their own antiparticle. Both possibilities allow for neutrino mass terms.

Unification of gauge couplings

Heisenberg's uncertainty principle states that $\Delta t \Delta E \geq \frac{\hbar}{2}$ and thus allows for violation of energy conservation for a short period of time. In QED, this results in vacuum polarizations of the photon propagator meaning that fermion-antifermion pairs in loops can exist as shown in Fig.6.

These loop corrections can be interpreted as fermion-antifermion pairs screening the charge which in turn can be understood as an energy dependence of the coupling. Accordingly, the QED coupling α_1 increases with increasing energy. To illustrate this, the values of α_1^{-1} are shown at the scale of the electron mass and the mass of the Z boson

$$\alpha^{-1}\left(m_e^2\right) = 137.035999084 \pm 0.000000051 > \alpha^{-1}\left(M_Z^2\right) = 128.95 \pm 0.05. \tag{42}$$

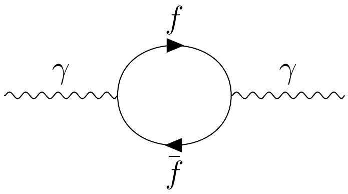

Figure 6: QED loop correction with f being any fermion

The qualitative behavior of the strong coupling g_s and the weak coupling g' is exactly opposite: for increasing energy the couplings decrease. In QCD this is in line with the confinement of the quarks as the force becomes ever stronger when the distance between the quarks is increased, so it is not possible to separate them. When extrapolating the energy dependent behaviour of the gauge couplings to very high energies, they almost intersect in one point as shown in the left plot of Fig.7.

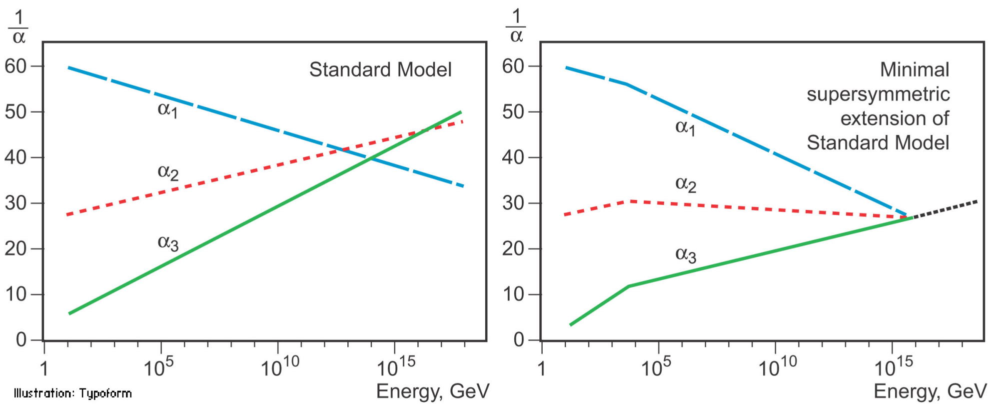

Figure 7: The running gauge couplings with α_1 being the electromagnetic gauge coupling, α_2 the strong gauge coupling and α_3 the weak gauge coupling. Figure taken from [25].

Although this is not necessarily a flaw in the theory it is assumed that there should be a theory predicting a unification of the gauge couplings at very high energies. An example for such a theory is supersymmetry (SUSY) which modifies the energy dependent behaviour of the gauge couplings in such a way that they do intersect in one point, shown in the right plot of Fig.7. No observations confirm any prediction made by SUSY so far and it remains unresolved whether it is realized in nature. More details on SUSY can be found in section 3.

Hierarchy problem

The problem of the large discrepancy between the energy scales of the different forces is generally known as the hierarchy problem. The electroweak scale is defined by the masses of the electroweak bosons which are $\mathcal{O}(10^2)$ GeV. On the other hand, gravitational effects become relevant at the Planck scale $(\hbar c/G)^{\frac{1}{2}} \approx 10^{19}$ GeV, where G is the gravitational constant. Therefore, the Planck scale defines the maximal scale up to which the SM is valid.

The nature of the problem becomes apparent when considering the Higgs mass. Additionally to the bare mass of the particle, there are correction terms coming from the other particles. The mass of the Higgs can therefore be written as:

$$m_H^2 = m_0^2 + \delta m^2 \tag{43}$$

where m_0^2 is the bare mass of the Higgs and δm^2 is the correction term. Like the QED loop corrections mentioned before, there are also such loop correction terms for the Higgs mass. In the SM the largest of such corrections is coming from the top quark as it is the most massive particle. Fig.8 shows the Feynman diagram of such a correction.

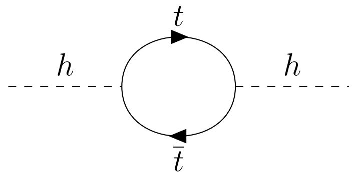

Figure 8: Higgs mass loop correction by the top quark

These corrections depend quadratically on the cutoff scale Λ which provides the upper bound for energies included in the loop integrals:

$$\delta m^2 \sim \Lambda^2. \tag{44}$$

In the SM, Λ is in principle not restricted but it has to be fixed to obtain a finite value for the Higgs mass. However, when Λ is set to the Planck scale, we obtain very large correction terms. In order to obtain the experimentally measured value of the Higgs mass in the SM, one then needs to set its bare mass to a negative value that exactly cancels these large corrections. This is called fine tuning. Instead of having to make use of fine tuning it would be preferable to have a theoretical justification for the relatively small value of the Higgs mass.

SUSY also offers an interesting solution for this problem. The loop correction terms have opposite signs for fermionic and bosonic particles. As SUSY predicts a fermion partner for every boson in the SM and a boson partner for every fermion the corrections would be cancelled by the corresponding partner. However, as stated before, no SUSY particles have been observed yet. This means that the symmetry must be broken since otherwise the supersymmetric partners would have the same masses as the SM particles.

Dark matter

Apart from the visible matter we observe there is experimental evidence for the existence of matter with quite different properties called dark matter. Detailed explanations on dark matter can for example be found in [26].

Early evidence for dark matter was observed by Fritz Zwicky in 1933 when he investigated the Coma galaxy cluster. He estimated the total mass of the cluster in two distinct ways, from the motion of some of the galaxies and from the brightness. When finding that these two values differed significantly, he suggested the existence of some form of additional mass that could not be detected so far which he called dark matter. Vera Rubin's investigations of galaxy rotation curves, carried out in the 1960's, gave further strong evidence of the existence of dark matter. She measured their rotation velocities, deduced their mass from it and again compared the result to the mass inferred from the brightness. With these very detailed measurements she confirmed the observations from Fritz Zwicky. Her findings have led to a great acceptance of the concept of dark matter.

Gravitational lensing effects also support the theory of dark matter. As a direct consequence of Einstein's theory of general relativity very massive objects such as galaxy clusters bend the light coming from the source to an observer in a way similar to an optical lens. The strength of the lensing effects observed for specific objects requires the objects to be more massive than can be deduced from the visible matter.

One can then deduce the distribution of the total energy density of the universe from these observations and additional evidence, such as the analysis of anisotropies in the cosmic microwave background (CMB) and studies of type Ia super novae. Only about 5% of the universe's total energy is made up of visible matter described by the SM while 25% is given by dark matter and the remaining 70% by dark energy. Dark energy explains the expansion of the universe but even less is known about it compared to dark matter.

While the existence of dark matter is widely accepted and stringent experimental evidence was found, its nature remains unknown. Many experiments are carried out in order to understand the nature of dark matter. First ideas suggested that the missing mass could be explained by non-luminous astrophysical objects like black holes or brown dwarfs. Especially primordial black holes that formed in the early universe could provide an explanation for the observations associated with dark matter. Although primordial black holes are still viable candidates to explain the dark matter, also possibilities of a particle-like dark matter are considered. When neutrinos were detected it was also thought that they could explain the unobserved mass but they travel at relativistic velocities and hence would not have allowed for galaxy formation. There are also continuous efforts to modify Newtonian gravity in such a way that it is able to explain the observed effects [27]. Although such an explanation could not be ruled out by now, the most popular idea remains to describe dark matter with one or several new, yet unobserved, particles. Such a particle should interact with the SM particles via gravity and if at all very weakly through other forces. It should be stable on the order of the lifetime of the universe, otherwise it would have decayed by now. Also, its total mass should be able to account for the amount of invisible mass as concluded from the observations. With these requirements there remain many possibilities for the properties of such a particle and many experiments search for different candidates.

SUSY provides a particle that fulfills all the requirements but there are many other candidates like the large group of Weakly Interacting Massive Particles (WIMPs) or an additional spin-0 particle called axion.

3 Supersymmetry

As already mentioned before, SUSY offers solutions to some of the shortcomings of the SM. It is therefore a strongly motivated theory for new physics and was eagerly awaited to be discovered at the LHC. For this reason a strong focus was put on SUSY searches at the LHC. However, no evidence of SUSY has been seen in any experiment so far and the results presented by the collaborations push the lower bounds for the masses still allowed for SUSY particles higher and higher. Nonetheless, it is not ruled out and the many results setting boundaries can be used to constrain SUSY. For reference, detailed explanations of the basic concepts of supersymmetry can be found in [28]. The particle content of the Minimal Supersymmetric Standard Model (MSSM) is presented here as more complex supersymmetric models do not lie within the scope of this thesis.

Since the tool `SModelS` which is subject of this thesis makes use of experimental results presented in form of so-called simplified models (see section 5.1) and most of these searches have been carried out in the scope of SUSY, its main ideas and concept will be briefly presented in this section. It should be stressed here that even though the `SModelS` database consists of SUSY results only it is capable of constraining other theories as well.

3.1 Particles in the Minimal Supersymmetric Standard Model (MSSM)

As briefly described earlier SUSY is motivated by its possibilities to solve two of the most important shortcomings of the SM, the hierarchy problem and dark matter, even though it was not originally developed as a solution to these problems. SUSY predicts a bosonic partner for every fermion and a fermionic partner for every boson. It therefore changes the spin of a particle by $\frac{1}{2}$ which is realized by an operator Q to generate the transformations

$$Q|\text{ Boson }\rangle = |\text{ Fermion }\rangle, \quad Q|\text{ Fermion }\rangle = |\text{ Boson }\rangle. \tag{45}$$

To describe single particle states in a supersymmetric model one uses the irreducible representations of the supersymmetry algebra called supermultiplets. The bosonic and fermionic states of a particle form such a supermultiplet. Each of the states is equivalent to a combination of the Q and $Q^\dagger$ operators acting on the other state up to a spacetime rotation or translation. As the operators Q and $Q^\dagger$ and all spacetime rotations and translations commute with the squared-mass operator $-P^2$ the two states of the same supermultiplet have the same eigenvalues of $-P^2$, so the same masses. Furthermore, Q and $Q^\dagger$ also commute with the generators of the gauge transformations. Thus the bosonic and fermionic states of the supermultiplet also have the same electric charge, color dimension and weak isospin. Additionally, the number of bosonic degrees of freedom is equal to the number of fermionic degrees of freedom in a supermultiplet.

The simplest realization of such a supermultiplet contains a single Weyl fermion[1] with two spin helicity states and two real scalars which can be combined to a complex scalar field. This is called a chiral supermultiplet.

The next-simplest possibility for a supermultiplet is called a vector supermultiplet. It consist of a massless (before gauge symmetry breaking) spin-1 vector boson with two helicity states and a spin-$\frac{1}{2}$ fermion. A spin-$\frac{3}{2}$ fermion cannot be the superpartner of a spin-1 vector boson as it would lead to a non-renormalizable theory.

To fit the observed SM particles into these supermultiplets it is important to note that chiral multiplets allow for different transformations for left- and right-handed fermions. Since this behaviour has been observed for all fermions of the SM they must be parts of chiral supermultiplets. Since the bosonic partners in the chiral supermultiplets are real scalars, the superpartners of the SM fermions have to be spin-0 bosons and not spin-1.

[1] A Dirac spinor can be written in terms of two Weyl spinors as $\psi = \binom{\psi_L}{\psi_R}$

The superpartners of the leptons and quarks are accordingly called 'scalar leptons' or short 'sleptons' and 'scalar quarks' or 'squarks'. They are denoted by the symbol of the corresponding SM particle with a tilde, e.g. $\tilde{u}_L$ and $\tilde{u}_R$. The handedness denoted for the supersymmetric partners does not describe their own helicity properties as they are spin-0 particles but represents the handedness of the corresponding SM particles. The squarks and sleptons have the same gauge interactions as their superpartners.

Since the Higgs boson is a spin-0 particle it has to be part of a chiral supermultiplet and it turns out that there even have to be two Higgs chiral supermultiplets to avoid inconsistencies in the electroweak gauge theory. There is one Higgs chiral supermultiplet H_u with hypercharge $Y = +\frac{1}{2}$ giving mass to up-type quarks which have an electric charge of $+\frac{2}{3}$. In addition there is another Higgs chiral supermultiplet H_d with hypercharge $Y = -\frac{1}{2}$ that gives mass to down-type quarks with an electric charge of $-\frac{1}{3}$. The name of the fermionic superpartners of the SM bosons is the name of the SM particle plus 'ino' at the end, so the superpartners of the Higgs boson scalars are called higgsinos and are Weyl spinor doublets.

The chiral supermultiplets are summarized in Tab.2.

	symbol	spin-0	spin-$\frac{1}{2}$
three families of (s)quarks	Q	$(\tilde{u}_L\, \tilde{d}_L)$	$(u_L\, d_L)$
	$\bar{u}$	$\tilde{u}_R^*$	$u_R^\dagger$
	$\bar{d}$	$\tilde{d}_R^*$	$d_R^\dagger$
three families of (s)leptons	L	$(\tilde{\nu}_L\, \tilde{e}_L)$	$(\nu_L\, e_L)$
	$\bar{e}$	$\tilde{e}_R^*$	$e_R^\dagger$
Higgs(ino)	H_u	$(H_u^+\, H_u^0)$	$(\tilde{H}_u^+\, \tilde{H}_u^0)$
	H_d	$(H_d^0\, H_d^-)$	$(\tilde{H}_d^0\, \tilde{H}_d^-)$

Table 2: The chiral supermultiplets of the MSSM

The vector gauge bosons of the SM are contained in vector supermultiplets and their superpartners are called gauginos. For the strong force there is the gluon with its superpartner the gluino. The gauge bosons of the electroweak force are the W^+, W^0, W^- and B^0 and their superpartners are called winos and bino. The physical mass eigenstates Z_0 and γ arise after electroweak symmetry breaking and are mixtures of the gauge eigenstates W^0 and B^0. The mixings of the corresponding supersymmetric particles $\widetilde{W}^0$ and $\widetilde{B}^0$ are called zino $\widetilde{Z}^0$ and photino $\tilde{\gamma}$. They would be mass eigenstates if SUSY was unbroken. The vector supermultiplets are summarized in Tab.3.

Names	spin-$\frac{1}{2}$	spin-1
gluon, gluino	$\tilde{g}$	g
winos, W bosons	$\tilde{W}^\pm$,$\tilde{W}^0$	$W^\pm$,W^0
bino, B boson	$\tilde{B}^0$	B^0

Table 3: The vector supermultiplets of the MSSM

The supermultiplets presented in Tab.2 and Tab.3 make up the particle content of the MSSM. As no SUSY particles with the same masses as their SM superpartners were found, SUSY would have to be a broken symmetry. In that case the SUSY particles could have large masses and therefore could not be produced with the energy available at the LHC today.

3.2 Supersymmetry breaking

When introducing supersymmetry breaking it is important to still allow for a solution of the hierarchy problem as this is one of the greatest assets that SUSY has. By introducing the superpartners of the fermion fields it is possible to cancel the problematic terms proportional to the square of the scale. To keep this intact, one can consider "soft" symmetry breaking and write the Lagrangian in the form

$$\mathcal{L} = \mathcal{L}_{\text{SUSY}} + \mathcal{L}_{\text{soft}}. \tag{46}$$

$\mathcal{L}_{\text{SUSY}}$ contains all terms of the gauge and Yukawa interactions and $\mathcal{L}_{\text{soft}}$ violates supersymmetry. In $\mathcal{L}_{\text{soft}}$ the largest scale is denoted as m_{soft}. The additional correction terms for the Higgs mass must be of the form

$$\Delta m_H^2 \approx m_{soft}^2 \, ln\left(\frac{\Lambda}{m_{soft}}\right) \tag{47}$$

so they do not cause problems regarding the hierarchy problem.

Furthermore, one can also find a justification for why the superpartners should be much heavier than their SM counterparts. The SM particles except for the Higgs only obtain their masses after electroweak symmetry breaking. For their superpartners the exact opposite is true and they can have a Lagrangian mass term in the absence of electroweak symmetry breaking. The squarks, sleptons and the Higgs scalars are all complex scalar fields and the corresponding mass term is allowed by the gauge symmetries. The higgsinos and gauginos are fermions in the real representation of the gauge group and can therefore be massive.

3.3 Mixing of gauginos and higgsinos

Another important consequence of electroweak and supersymmetry breaking is that the superpartners listed before are not necessarily the mass eigenstates of the theory. Instead there can be mixing of the electroweak gauginos and higgsinos and between sets of squarks and sleptons that have the same electric charge. The gluino does not have appropriate quantum numbers to mix with any of the other particles. For sfermions this means that they can be split into right-handed and left-handed parts while the gauginos and higgsinos form new mass eigenstates called neutralinos denoted by χ_i^0 (i=1,2,3,4) and charginos $\chi_j^\pm$ (j=1,2). The resulting mass eigenstates are summarized in Tab.

	spin-0	spin-$\frac{1}{2}$
three families of (s)quarks	$\tilde{u}_{L,R}$, $d_{L,R}$	$u_{L,R}$, $d_{L,R}$
three families of (s)leptons	$\tilde{\nu}_L$, $\tilde{e}_{L,R}$	ν_L, $e_{L,R}$
Gauge(inos) and Higgs(inos)	$h^0, H^0, A^0, H^\pm, W^\pm, Z^0$	$\tilde{\chi}_1^0, \tilde{\chi}_2^0, \tilde{\chi}_3^0, \tilde{\chi}_4^0, \tilde{\chi}_1^\pm, \tilde{\chi}_2^\pm$
Alternative notation for gauginos and higgsinos		$N_1, N_2, N_3, N_4, C_1^\pm, C_2^\pm$

Table 4: The mass eigenstates of the MSSM

3.4 R-parity

The MSSM is a viable new physics theory, however, it also allows for additional terms that contradict observations. It is possible to construct gauge invariant terms that violate lepton or baryon number conservation but no such decays have been seen so far. By allowing these terms, it would be possible to have a rapid proton decay mediated by a squark, for example $p \to e^+\pi^0$ mediated by a strange or bottom squark. These operators are highly constrained via experimental observations that set the lower limit of the lifetime of the proton to $> 1.6 \times 10^{34}$ years [29].

To avoid these decays a new symmetry is introduced which is a discrete Z_2-symmetry[2] called R-parity and is defined as

$$P_R = (-1)^{3(\mathrm{B-L})+2s}, \tag{48}$$

where B is the baryon number, L the lepton number and s the spin of the particle. R-parity is a multiplicatively conserved quantum number. Since R-parity depends on the spin, all SM particles and the Higgs bosons have even R-parity ($P_R = +1$) and all squarks, sleptons, gauginos and higgsinos have odd R-parity ($P_R = -1$). This has several interesting phenomenological consequences. The lightest supersymmetric particle (LSP) has to be stable because a SUSY particle decaying to a SM particle would violate R-parity. If this particle was neutral, it would be a good candidate for a dark matter particle. Another consequence of R-parity is the production of sparticles in colliders in even numbers only.

3.5 Searches for sparticles at the LHC

Due to R-parity, the supersymmetric particles are typically assumed to be produced in pairs. In proton-proton colliders like the LHC, the sparticles would be produced either via the strong or the electroweak interaction. By interaction via the strong force the quarks and gluons could produce a pair of their corresponding superpartners, leading to processes like $qq \to \widetilde{q}\widetilde{q}$, $gq \to \widetilde{g}\widetilde{q}$ or $gg \to \widetilde{g}\widetilde{g}, \widetilde{q}\overline{\widetilde{q}}$. The production processes via the electroweak interaction include $q\overline{q} \to \widetilde{\chi}^{\pm}\widetilde{\chi}^{\mp}, \widetilde{\chi}_2^0\widetilde{\chi}_2^0, \widetilde{\ell}^{\pm}\widetilde{\ell}^{\mp}, \widetilde{\nu}_L\widetilde{\nu}_L$ and $u\overline{\mathrm{d}} \to \widetilde{\chi}^{+}\widetilde{\chi}_2^0, \widetilde{\ell}_L^{+}\widetilde{\nu}_L$.

The decay chains of the sparticles have to end in the LSP again to conserve R-parity. The LSP is typically the lightest neutralino $\tilde{\chi}_1^0$ which is charge and color neutral. For all further discussions it is assumed that the $\tilde{\chi}_1^0$ is the LSP. These decays could take place directly where the produced SUSY particle decays into the LSP and SM particles as in $\widetilde{\ell} \to \ell\widetilde{\chi}_1^0$. Decays with several steps until the LSP is reached are called cascade decays like the decay $\widetilde{\ell} \to \ell\widetilde{\chi}_2^0, \widetilde{\chi}_2^0 \to \ell^+\ell^-\widetilde{\chi}_1^0$. Here, the slepton needs to be heavier than the $\widetilde{\chi}_2^0$ to allow for the decay to take place.

Experimental signals

In LHC searches for decays with the LSP in the final state, the missing energy transverse to the beamline (MET) is determined per event which is denoted as $\not{E}_T$. A general signature of SUSY could be described as n leptons + m jets + $\not{E}_T$, where n and m represent the number of leptons or jets respectively including 0. There are of course SM processes with similar signatures which are the background for such possible signals. Especially processes involving Z or W bosons are relevant backgrounds as they often include neutrinos which also appear as missing energy in the detectors. To reduce these backgrounds, cuts in kinematic observables are applied in the searches. These cuts depend on the properties of the SUSY particles being searched for. In order to cover broad ranges of properties like the mass, different cuts are applied which define different signal regions. One classic SUSY search is for example looking for events with jets and $\not{E}_T$ but no energetic lepton. The remaining electroweak background contributions include $Z + jets$ with Z decaying as $Z \to \nu\overline{\nu}$ in addition to QCD backgrounds.

In the past decade a very large number of such decays was covered by experimental analyses setting lower limits on the masses of the SUSY particles. Many channels with MET final states have been exhaustively investigated, so it has become necessary to investigate more complex signatures as well. One large group of these signatures that do not include $\not{E}_T$ in the final state will be presented in the next section.

[2] Z_2 is the cyclic group of order 2. It consists of two elements a and b that satisfy $ab = ba = a$ and $a^2 = b^2 = b$. An example is the multiplicative group formed by 1 and -1.

4 Long-lived particles

In the search for new physics, there has been a strong focus on missing energy searches ever since the LHC was built. Decays with missing energy signatures result from prompt decays of BSM particles into SM final states plus charge and color neutral LSPs. When ATLAS and CMS were built it was expected to see new physics in these prompt decays. New particles were thought to be very heavy compared to SM particles and so unstable that they decay very quickly. Therefore, most searches were focused on decays with missing energy. In such decays, there is too little energy and momentum in the final states compared to the initial states. Due to energy and momentum conservation of the decay the energy must be carried away by the stable neutral particle. SUSY that conserves R-parity (see section 3) leads exactly to such signatures. It was widely expected in the community that discoveries of SUSY particles would be made with the LHC. Recently, as we continue to see no prominent excess in missing energy searches for new physics, more exotic signatures are considered in both the experimental and theory community. One group of such signatures are the long-lived particles (LLPs). Long-lived particles are particles other than the LSP that do not decay right after being produced but have a macroscopically detectable decay length. This includes particles that just survive the innermost detector but also particles that decay far outside of the detector. Long-lived particles can then lead to distinct signatures like decays within the detector or charged tracks with large energy loss which can be distinguished from traces left by SM particles. Even though the detectors at the LHC were originally not aimed at these signatures they are also capable of detecting such long-lived particles.

A detailed review of long-particles including theoretical motivations and the current status of searches for LLPs at the LHC and other colliders can be found in [30].

4.1 Theoretical motivation

Long-lived particles appear in theories with degenerate mass spectra or suppressed couplings. The proper lifetime τ of a particle is defined as:

$$\tau^{-1} = \Gamma = \frac{1}{2m_X} \int d\Pi_f \left|\mathcal{M}\left(m_X \to \{p_f\}\right)\right|^2 , \tag{49}$$

with m_X being the mass of the decaying particle, $\mathcal{M}$ the matrix element of the decay, $\{p_f\}$ the decay products and the phase-space of the decay $d\Pi_f$. The inverse of the proper lifetime τ is the decay width Γ. In order for a particle to have a long lifetime and so a small decay width either the phase space or the matrix element must be small. A small matrix element results for example from an approximate symmetry. If it were exact the operator mediating the decay would be forbidden but in case of small symmetry breaking it leads to a small coupling constant of the operator. It can also be realized by an effective higher dimension operator which leads to a suppression of the coupling constant. A small phase-space can also result from small breaking of an approximate symmetry. It can furthermore arise from accidental degeneracies in the spectrum.

Generally speaking, a suppressed decay appears in models with one of the following features. In models with (nearly) degenerate mass spectra the mass difference between the parent and the child particle is small which decreases the probability for this decay to take place. Small couplings lead to a decay that is inherently less likely to happen. Highly virtual/heavy intermediate states suppress the decay as more energy is needed to produce such an intermediate state.

In the SM there are many particles with long lifetimes which origin from the mechanisms outlined before. For example, the proton has an extremely long lifetime of $> 1.6 \times 10^{34}$ years [29]. An approximate symmetry gives rise to this long lifetime: baryon number conservation which is an accidental symmetry of the Standard Model. The μ also has a long lifetime of about 2×10^{-6} s [7] due to its small coupling arising from the high mass of the W boson. As there are many examples for particles with long lifetimes in the SM, it does not seem surprising that such particles may also exist in models beyond the Standard Model. Many BSM theories including SUSY, models predicting dark matter particles or models with portals to hidden sectors predict long-lived particles. Some examples for models leading to long-lived particles in SUSY will be given here, further details on these SUSY models and other theories leading to long-lived particles can be found in [31].

Long-lived particles in SUSY

Within SUSY there are several possibilities to obtain long-lived particles.
In general it is possible within the MSSM to have particles with long lifetimes with a suitable hierarchy of the SUSY particles. For example, if the lightest chargino and neutralino are near mass degenerate the chargino can have a long lifetime.

Another possibility for long lifetimes in the MSSM occurs when the gravitino, the supersymmetric partner of the hypothetical graviton, is the lightest SUSY particle (LSP). In this case the mass of the gravitino and its coupling to the next to lightest SUSY particle (NLSP) solely depend on the scale of SUSY breaking. It turns out that for this scale there exists a range such that the gravitino mass is small and the coupling suppressed which leads to a long lifetime of the NLSP. This mechanism is called Gauge Mediated SUSY breaking (GMSB) [32].

A different example for an extension of the MSSM leading to macroscopic decay length is R-parity violation (RPV) [33]. RPV operators are in general highly constrained as they have to avoid the typical drawbacks that arise without R-parity conservation like rapid proton decay. Consequently, the couplings are generally small when SUSY particles decay via an RPV operator which leads to long lifetimes.

Furthermore, models of split SUSY can also lead to long-lived particles. Split SUSY predicts a breaking of supersymmetry at extremely high scale. It therefore gives an explanation for the fact that no SUSY particles have been observed. Furthermore, it also avoids proton decay. It predicts that most SUSY particles including the squarks have very large masses but due to chiral symmetries, the fermions and especially the gluino can have masses of the order of the weak scale. As the squarks have very high masses and direct decay to colored particles of the SM is not allowed due to R-parity conservation, the decays of the gluino are largely suppressed and lead to a long lifetime.

4.2 Detector signatures of long-lived particles

From the experimental point of view, long-lived particles can be categorized depending on their travelled distance and their behaviour inside of the detector. Fig.9 shows a cross-sectional view transverse to the beam direction of how different signatures would appear in a detector.

The different signatures are presented in this section. A very brief overview of the general composition of an LHC detector is given to explain how LLPs would appear in the detectors. No specific detector is described or displayed in the figures of this section. Instead, the most important subsystems that most high energy collider detectors today have in common and their basic functionality are presented.

In general, one distinguishes between direct and indirect detection techniques. Direct detection means measuring the interaction of the particle with the detector material as is the case when measuring anomalous inoization. Indirect detection means reconstructing the decay to SM particles which is for example applied when searching for displaced vertices.

Long-lived particles could be identified by leaving characteristic signatures in different parts of the detector and can so be distinguished from SM particles.

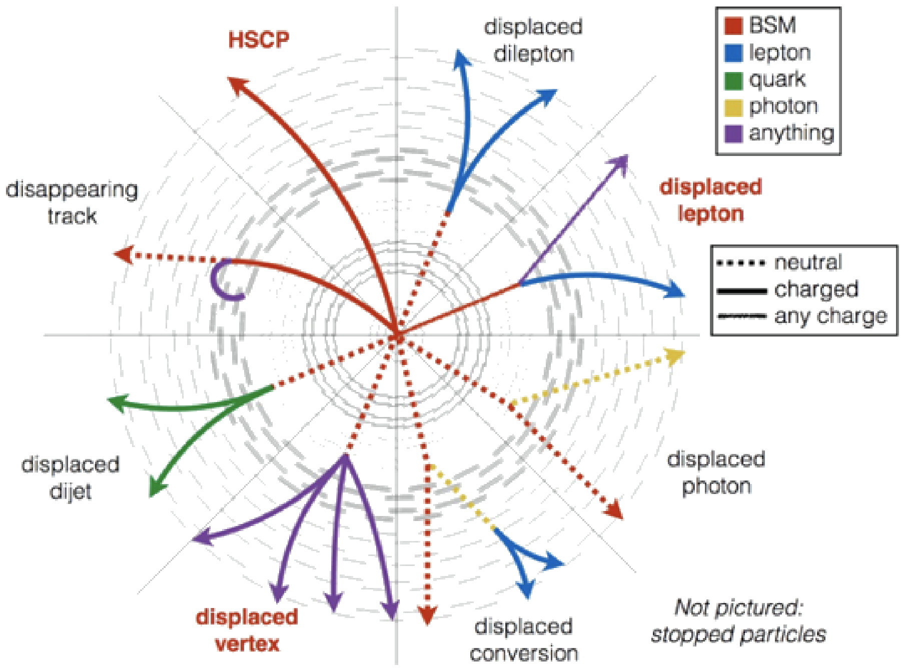

Figure 9: Different detector signatures for long-lived particles; image taken from talk by J.Antonelli at ICHEP 2016.

4.2.1 A general collider detector

Detectors of high energy colliders all have a similar principle structure. They consist of several layers to optimally measure the properties of different particles. A schematic illustration of a general collider detector with the most important layers is shown in Fig.10.

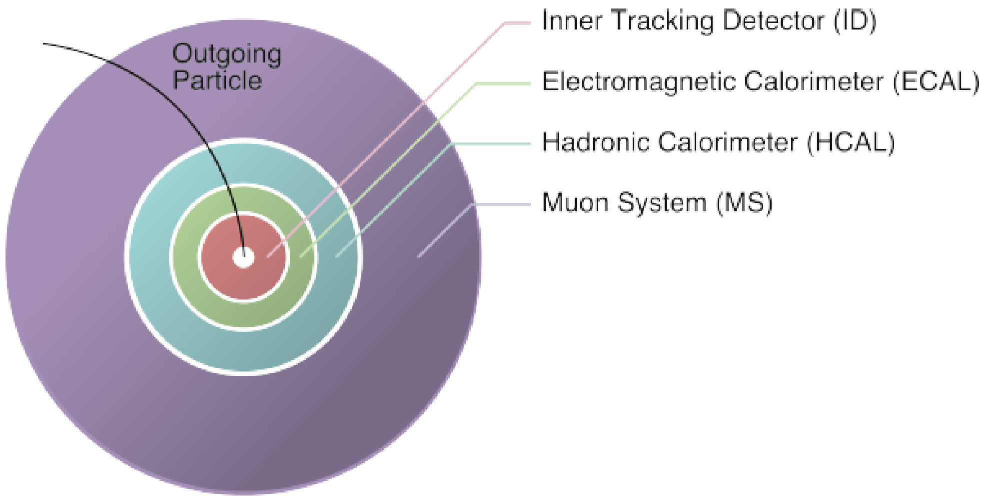

Figure 10: A schematic illustration of a collider detector, figure taken from [30].

The inner detector (ID) can detect electrically charged particles that travel through it. In the SM, the particles typically measured by the ID are leptons, like the electrons and muons and hadrons like the charged pions and kaons and the proton. The ID measures the ionization of these particles in a gaseous or solid-state detector and then registers a hit. This gives the trajectory of the particle called a track. The ID is therefore also called the tracker. Placed in a magnetic field, the momentum and electric charge of the particle can be inferred from the direction and curvature of the track.

The next layer is the electromagnetic calorimeter (ECAL) which measures the energies of electrons, positrons and photons. The energy is measured from the interactions of these particles with the detector material via e^+e^--production and photon radiation. These interactions are then measured, for example with scintillators where the photons excite the molecules of the material which then emit light when returning to the ground state.

The hadronic calorimeter (HCAL) is dedicated to measuring the energies of hadrons. Quarks and gluons form sprays of hadrons called jets which are detected by this detector in addition to the ECAL. The principle by which it detects the particles is similar to that of the ECAL but it is specifically built to detect collections of particles. Therefore it is ideal for detecting jets.

The outermost layer is the muon system (MS). Muons are heavy enough to only lose little energy via ionization and are therefore capable of travelling through the calorimeters. The MS is oftentimes also placed in a magnetic field in order to measure the momentum of the muons. By combining this information with the information obtained with the ID one gets high resolution momentum measurements.

The collider detectors were originally designed to optimally measure the SM particles produced in SM processes or prompt decays of BSM particles. Nevertheless, since LLPs can interact in similar ways with the detector material they could also be measured with the existing detectors. Because they have long lifetimes and are assumed to be heavy, their signatures would be distinct to those left by the SM particles. The different characteristic signatures will be outlined below. The LLPs can either give rise to one of these characteristic signatures or a combination of several which would give even more detailed information on the behaviour of an LLP.

4.2.2 Anomalous Ionization

Charged LLPs could be identified in the ID by their characteristic track. If there are indeed heavy charged particles, they could be characterized by a large energy loss. A particle significantly heavier than a standard model particle would consequentially be traveling at a lower speed since the total available energy is limited. The energy deposit depends on the speed and the charge of the particle according to the Bethe-Bloch-formula [7]:

$$\left\langle \frac{dE}{dx} \right\rangle \sim -\frac{z^2}{\beta^2} \cdot \left[\ln \left(\frac{\beta^2}{(1-\beta^2)} \right) - \beta^2 + C \right], \tag{50}$$

where the constant C depends on the detector material, z is the electric charge of the particle and β its velocity. For a particle that is either slow (compared to SM particles) or has a large z this energy loss would be exceptionally large and therefore detectable. This anomalous ionization can be detected by the ID or the MS as they measure the charge deposition.

If these LLPs have especially large lifetime they could traverse the whole detector before decaying and therefore appear stable on detector scales. Such particles are called Heavy Stable Charged Particles (HSCP).

4.2.3 Delayed signals

A particle travelling significantly slower than a SM particle will arrive at the outer detector layers at a later time than the SM particle. Upon measuring this distinct signature one could then obtain the mass of the particle by measuring the time of flight in addition to the momentum. To measure this delay the detector subsystems need to have a high timing resolution. At the LHC bunch crossings are typically separated by 25 ns and the outermost detector subsystem, the muon system, has a timing resolution of $O(1)$ ns. With this resolution and the large distances between detector subsystems delayed signals can be measured with high precision.

If the particle becomes so slow that it gets stopped completely and also has a long lifetime it could decay outside of the triggering and readout time windows. These signals would be lost or misidentified with some later events. To be able to detect these signals as well, a dedicated trigger was developed at the LHC that makes use of so-called empty bunch crossings. If a decay took place during this bunch crossing, the signal could be seen as it would appear without background from a collision. Triggering on empty bunches gives the possibility to detect such LLPs.

4.2.4 Disappearing Tracks

Charged long-lived particles that enter the ID but decay within it could appear as a disappearing track if the decay products of such a BSM particle were very soft. As the soft decay products could not be tracked, the track of the initially produced particle would seem to disappear midway. As these tracks have only a few hits, the resolution of the momentum is lower than for complete tracks.

If exactly one of the decay products is hard enough to allow for reconstruction of its track, the signature would show two tracks connected at an angle. This is called a kinked track. Since a kinked track provides more information than a disappearing track the background can be reduced more efficiently.

4.2.5 Displaced Tracks and Displaced Vertices (DV)

Displaced tracks are tracks that do not seem to originate from the beam spot where the collision took place. They arise when an electrically neutral particle decays to charged particles within the detector after travelling a macroscopic distance. A characteristic measure for displaced tracks is the impact parameter d_0 which is the shortest distance in the (x, y) plane from the beam spot to the track. The spot where prompt tracks originate from is also called primary vertex (PV). At the LHC there are about 50 PVs per collision. The distance in the direction of the beam z_0 can also be measured but does not usually hold relevant information as for a hadron collider a large displacement in the z-direction can simply mean that it is originating from a different primary vertex. The displacement of a track is usually measured as $\frac{d_0}{\sigma_{d_0}}$ where σ_{d_0} is the uncertainty of the impact parameter. Dedicated searches have to be performed in order to reconstruct tracks with large displacement as most other searches are focused on prompt decays and therefore do not store information about events with large displacement.

One furthermore distinguishes between a displaced track and a displaced vertex. The latter is observed when several displaced tracks originate from the same point. Its distance to the primary vertex can be measured more precisely than for a displaced track as more tracks are involved.

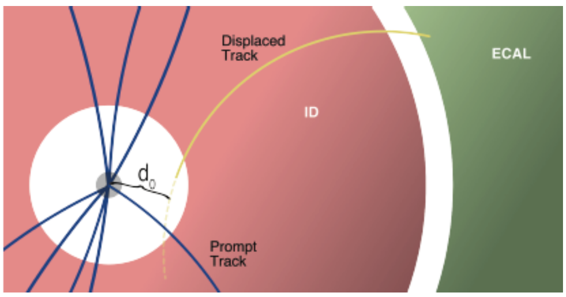

(a) Displaced Track

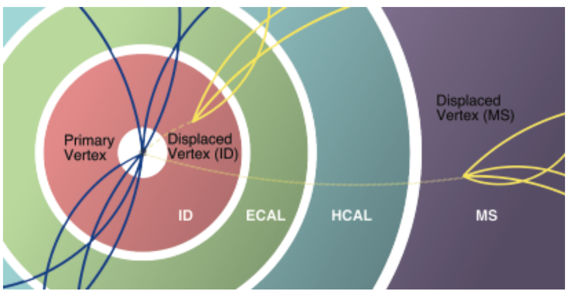

(b) Displaced Vertices

Figure 11: Prompt tracks in addition to a displaced track (11a) and displaced vertices (11b), figures taken from [30].

4.2.6 Displaced Calorimeter Deposits

Track reconstruction and a measurement of the displacement are typically limited to short distances of a few tens of cm as this is the typical size of the inner detector. Additionally, these measurements can only be performed for charged particles.

It is however also possible to detect larger displacements since the calorimeters of the detector can also be used to measure displacement. If a calorimeter has a three-dimensional segmentation it can detect the direction of the incoming particle which in turn determines d_0 and z_0. This technique is for example used to identify so-called non-pointing photons that originate from a displaced decay.

Within the scope of this thesis, the software tool `SModelS` was modified. It was extended to also be able to handle simplified model results from the LHC looking for signatures with long-lived particles as described in this section. In the following section, `SModelS` will be introduced. We first describe the version that only made use of MET results and continue with the changes necessary for results with long-lived particles.

5 The SModelS framework

No signs of BSM physics have been seen in experiments so far. Instead, the number of searches setting limits on the properties of potentially new particles increases continuously as does the number of theories for new physics. Both searches and theories have become ever more complex since the simpler models have been ruled out early on. With such a large amount of data to be compared to theoretical predictions, it has become a devious task to decide whether it is worth pursuing a new model or whether it has already been ruled out by an experimental result.

The open source software tool SModelS [34, 35] offers an approach to carry out this task. In a fast and model independent way, it compares new physics input theories[3] to simplified model results provided by the ATLAS and CMS experiment at the LHC at CERN. In this section, the concept of simplified model spectra will be introduced and the basic working principles of SModelS explained.

5.1 Simplified Model Spectra

A detailed introduction on the basic concepts of simplified models can be found in e.g. [36].
In the search for new physics at the LHC, the key approach is to compare data to new physics models. Looking at data distributions alone can provide important information about new physics and has lead to discoveries in forms of resonance measurements in the past. However, these options have been exhaustively explored and furthermore would only give little information on the complete BSM model. It has therefore become necessary to investigate other properties which do not lead to sharp features and are thus harder to determine.

It has become common practice to analyze the data with respect to a given theory model. Understanding the data in terms of theoretical models is generally known as interpretation. One possibility to interpret the data is in terms of a full model. Full model interpretations are very accurate but are limited in their application as they can only be used to constrain predictions of this one model. In order to broaden their application, alternatives to full model interpretations were developed. A critical quantity in this respect is the number of free parameters that the model has in terms of which the data is interpreted. Examples for the free parameters are the masses of the new particles and their branching ratios. It is therefore necessary to find a model that describes the data well and at the same time find an appropriate number of such free parameters. The number of degrees of freedom has to be large enough to interpret the data but the number of new particles should be small enough to make an analysis of the model feasible. An example for a full model with a large number of free parameters is the Minimal Supersymmetric Standard Model (MSSM) which has $\mathcal{O}(100)$ free parameters. An interpretation of the data in terms of the MSSM therefore has a large number of degrees of freedom. On the other hand when interpreting the data in terms of a model with only very few new particles, it is likely that only parts of the data can be described by that model. Nevertheless, interpretations in terms of models with few particles can be carried out more efficiently and thoroughly. Consequentially one has to find a compromise between the two extremes. Ideally, the model used to interpret the data would contain just enough parameters to allow for a discovery of new physics but no more. A more detailed description could then be obtained by consecutively introducing more particles.

Interpretation of experimental searches in terms of simplified model spectra (SMS) offers an alternative to the interpretation in terms of full models. They serve as an aid to discover more exact models while also providing an interesting tool for analysis in their own right. The number of new parameters for the simplified models is limited as the Standard Model (SM) is extended by only a few new particles, typically 2-4. The results of the searches can then be presented as a

[3]within the scope of SModelS a theory always refers to a set of fixed values for the model parameters like the masses of the new particles which is also referred to as model point

function of e.g. the masses of these new particles. In many cases, simplified models are the limits of more general models where the other particles are irrelevant for the analysis. Interpretations in terms of simplified models, from now on referred to as simplified model results, have an important advantage compared to interpretations in terms of full models. They cannot only be applied to constrain the exact same model but instead can be used to constrain many different full models which obey the same kinematics. Any full model can be understood as a collection of several simplified models and each of these can then be constrained by a simplified model result. It is however not straightforward to decompose a full model into simplified models and find the according simplified model results to constrain them. SModelS provides the missing link to achieve this in a fast and model independent fashion. It is, however, limited to models with a Z_2-symmetry (see section 3.4).

The database of SModelS consists of about one hundred ATLAS and CMS results which are presented in terms of simplified models. Every result in the SModelS database is defined by one simplified model. In SModelS it is assumed that the results of experimental searches for new physics only depend on the event kinematics and are independent of the quantum numbers of the BSM particles like electric or color charge. To characterize an event, one then only needs the event topology, so the number of vertices and the SM final states, the event weight as a product of the production cross section and the branching ratio ($\sigma \times BR$) and the masses of the new particles.

For notation, a full model Feynman diagram can be reduced to a simplified model representation. An example is shown in Fig.12. The protons as well as the W are summarized in an effective vertex and only directly observable SM particles remain. The new particles are removed to symbolize that their specific properties are not relevant, only their masses are kept.

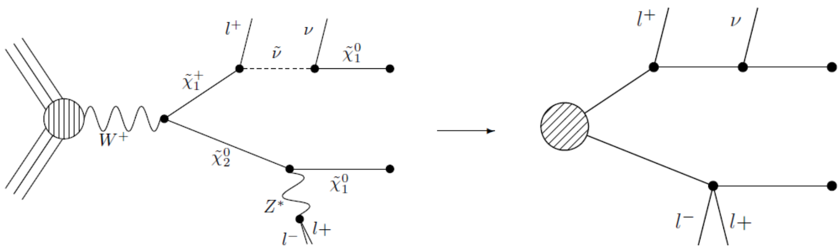

Figure 12: Feynman diagrams for a decay as full model and simplified model, figure taken from [34].

Typically the simplified model results are presented as a function of the masses of the new particles for one specific topology either as cross section upper limits or as efficiencies where the upper limit is given for the total signal of one specific signal region (see section 5.2.4). For example, constraints on squark pair production with $\widetilde{q} \to q + \widetilde{\chi}_1^0$ would be presented as functions of $(m_{\widetilde{q}}, m_{\widetilde{\chi}_1^0})$.

5.2 Basic principles of SModelS

SModelS decomposes a new physics model with a Z_2-symmetry provided by the user into simplified topologies and then compares these to its database of LHC simplified model results. The full theory model is constrained with simplified model results by matching different decay chains resulting from the full model to different simplified models from the database. Resulting from this comparison, the given theory gets constrained by the experimental results. Furthermore, SModelS also gives information on decay chains arising from the theory which have not been covered by experiments yet. Fig.13 shows the basic working principle of SModelS which will be outlined in the following. Further details on the procedure can be found in the `SModelS` documentation [35].

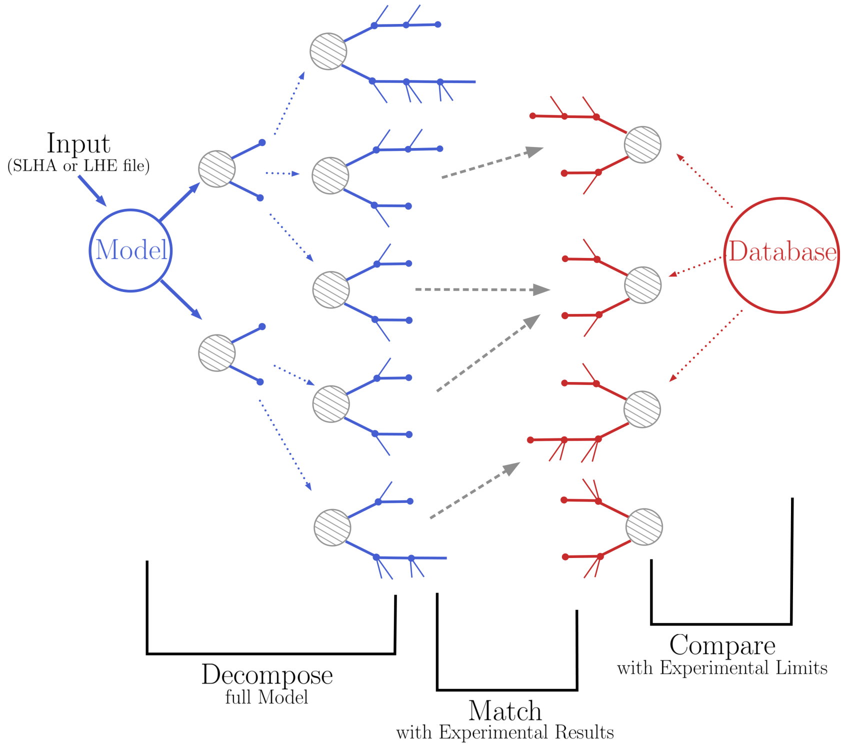

Figure 13: Schematic illustration of the working principles of `SModelS`, figure taken from [35].

As can be seen in Fig.13, the general procedure applied by `SModelS` brings together the theoretical input model (blue) and the experimental database (red).

5.2.1 Parameter file

`SModelS` also needs a parameter file in addition to the input file. The parameter file configures `SModelS`. If no parameter file is given, default settings are used. The user can either give a different parameter file or modify the one provided in order to suit their needs. Among the parameters that can be adjusted are the number of CPUs used for the calculation, the path to the database and the experimental results that should be used during the comparison (by default all results in the database). In addition one can also specify if the mass and invisible compression should be carried out when building the theory elements (see section 5.2.3). Furthermore, the minimum required cross section of an element can be set in the parameter file.

5.2.2 Terminology

A full decay chain like the one shown in Fig.12 is called an *element* in `SModelS`. It consist of two *branches* which is split up into several *vertices*. This structure is called a *topology* and is then dressed with the SM particles and the masses of the new Z_2-odd particles.

The *bracket notation* is introduced for convenient description of the elements. It represents the element with several nested brackets to include not only the particles but also the topology of the element in a single expression. Going from the outermost brackets to the innermost, they are organized as follows. For every *branch* there are brackets. The next brackets correspond to the vertices in each branch. Within these brackets the Z_2-even particles coming out of that vertex are listed. An example for the *bracket notation* is shown in Fig.14.

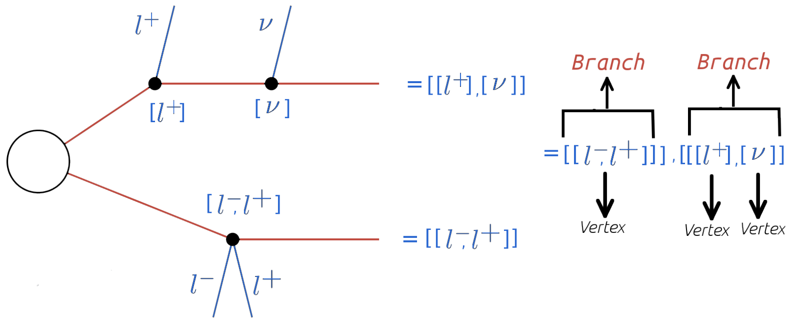

Figure 14: The bracket notation in SModelS, figure taken from [35].

5.2.3 Theory input

On the theory side the starting point is the theory input file. This is a full and complex BSM scenario with fixed values for the masses of the new particles, their production cross sections at LHC and their decay channels with corresponding branching ratios. It is often also referred to as a model point. It must be given in one of two standardized formats, the SUSY Les Houches Accord (SLHA) or Les Houches Event (LHE) data format. The core module of the theory part is the decomposition where the model defined in the file is decomposed into its decay chains.

Decomposition

The process of reading the input theory file and automatically computing all possible decay chains from it, is called decomposition in SModelS. The signal of the full model is hereby decomposed into simplified model topologies. As a first step the new particles and their properties are read in from the file. The masses, production cross sections and decay channels with branching ratios can be read off directly for SLHA files. LHE files on the other hand provide information on the individual events and their vertices, so for these files there are additional modules for reading and decomposing the file[4]. Next, the production cross sections are read. As the model must be Z_2-symmetric, the production cross sections are always given for pairs of new Z_2-odd particles. These two particles are the starting points of the two branches of the element (as shown in the very left part of Fig.15). For each of these particles the corresponding decay channels are read. The branching ratio for the decay and the particles it decays to are needed. For example, a gluino could have the two decays [0.5[1,-1,1000022], 0.5[2, -2,1000022]] listed in the file where the numbers in the inner brackets are the PDG numbers of the particles. This means that the gluino decays with a branching ratio of 0.5 to an $u\bar{u}$-pair (PDG 1 and -1) and the lightest neutralino (PDG 1000022) and with a branching ratio of 0.5 to an $d\bar{d}$-pair (PDG 2 and -2) and the lightest neutralino. Within the scope of SModelS, SM particles are always assumed to be final states. For the purpose of SModelS, it is therefore assumed that the branching ratio of all SM particles is 0, so they do not decay.

For every decay a new branch is created, resulting in a number of different decay chains for each branch. The resulting elements then consist of all possible combinations of the different decay chains for the two branches as in Fig.15.

Additionally, the production cross section is multiplied by the corresponding branching ratio (BR) for every decay in the element. This way the cascade decay is built up until the lightest supersymmetric particle (LSP) is reached. As a result, many different elements are produced

[4]There is a dedicated SLHA-decomposer and an LHE-decomposer because of the different formats. The procedure described here applies to the decomposition of SLHA files.

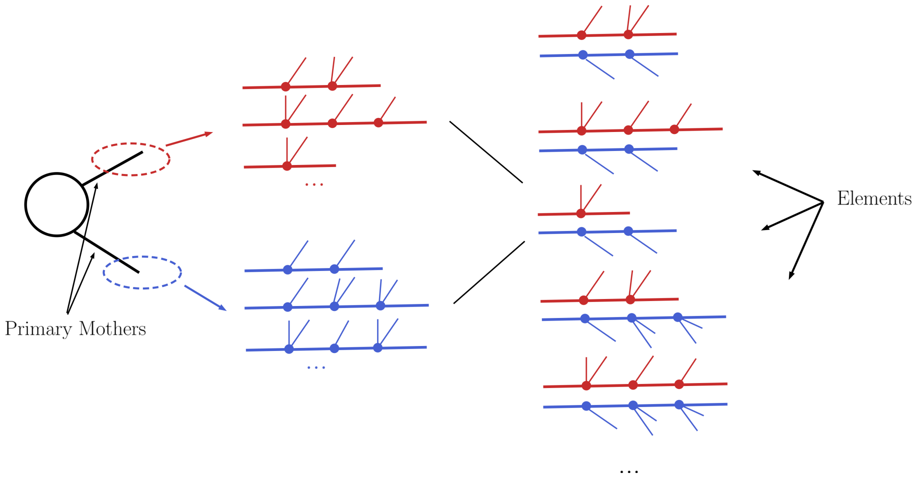

Figure 15: The SModelS decomposition procedure, figure taken from [35].

from all possible combinations of branches with different total cross sections

$$\sigma = \sigma_{production} \times \prod_i \mathcal{BR}_i, \tag{51}$$

where i goes over all vertices in the element.

Compression

To further simplify the resulting elements, two forms of compression are applied whenever the arising signatures allow. Compressing the element means to reduce the number of steps in the decay chain which is useful because it is then more likely to be constrained by an experimental result as these usually cover shorter rather than longer decay chains. However useful, it should be noted that the compression does lead to an approximation of the element.

Mass compression: If two particles are near mass degenerate a decay of the slightly heavier particle to the lighter one results in soft SM final states which cannot be detected. Therefore one can safely neglect this decay and only keep the lighter of the two masses as illustrated in Fig.16.

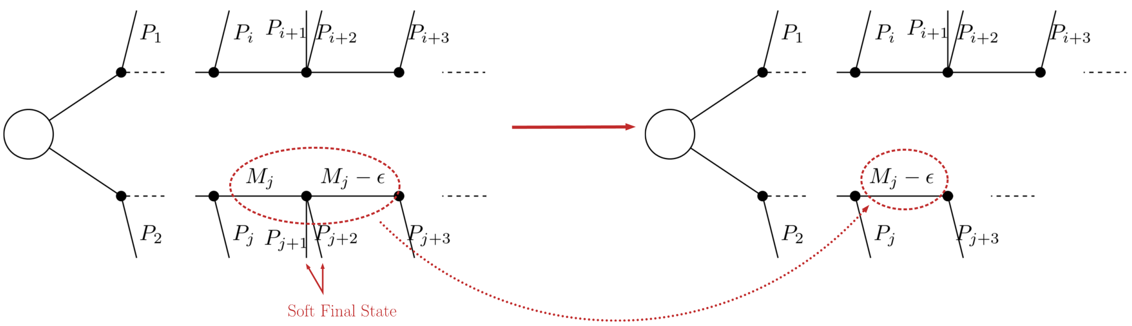

Figure 16: The mass compression of elements, figure taken from [35].

Whether the mass compression applies, is determined by the mass difference of the two particles. The maximum mass difference of two particles that leads to a compression of the element is by default set to 5 GeV but can be manually set by the user in the parameter file.

Invisible compression: An invisible compression applies if the last decay is invisible. This means that additionally to the invisible stable BSM particle in the final state also the last SM particle is invisible, e.g. a neutrino as in Fig.17.

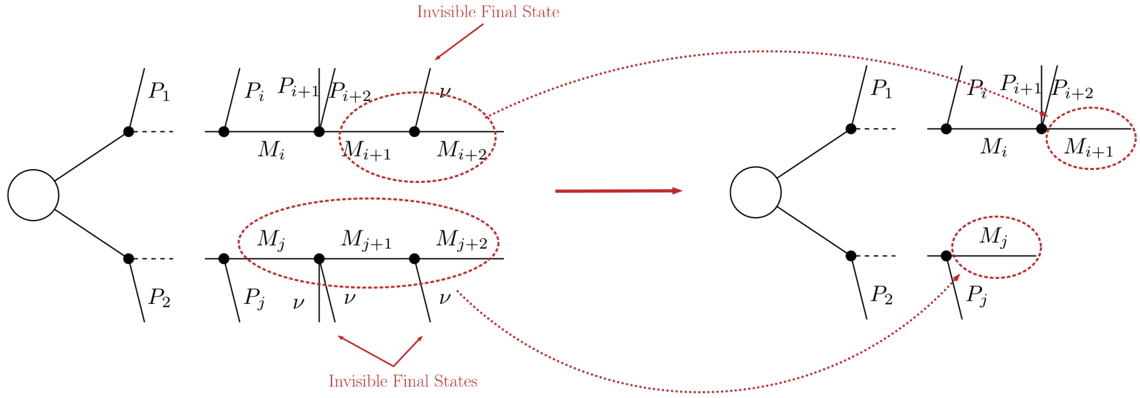

Figure 17: The invisible compression of elements, figure taken from [35].

Since neither the LSP nor the neutrino can be detected by the experiments, the resulting missing energy is equal to the sum of the energies of the two particles. This is equivalent to the energy of the next to last BSM particle and so the last vertex can be omitted.

5.2.4 Experimental database

The experimental results in the database are presented in form of an upper limit (UL) map or an efficiency map (EM).

Upper limit maps give the 95% confidence level upper limit on the cross section times the branching ratio $\sigma \times \mathcal{BR}$ and are provided by the experimental collaborations. They are calculated in the scope of simplified models, meaning they assume 100% branching ratio for the decay channel(s) investigated. They constrain a single simplified model topology and are given as functions of the masses of the different BSM particles involved. An example for an UL map is shown in Fig.18. It should be noted here that the exclusion curves shown in black and red in Fig.18 are not used by SModelS, only the underlying "temperature" map.

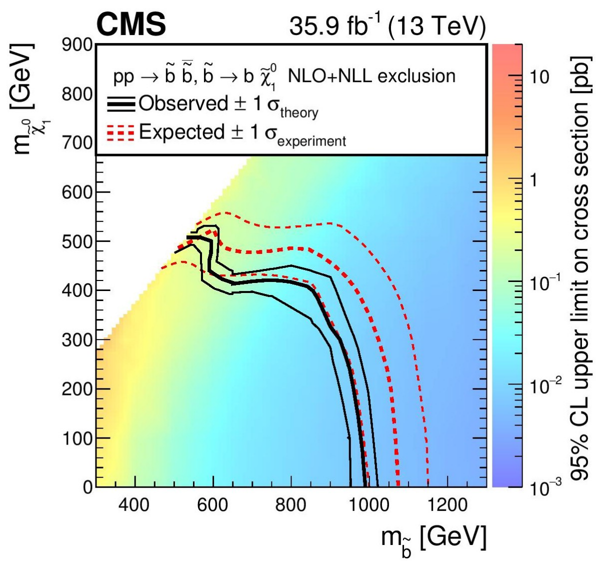

Figure 18: Upper limit map on the cross section from CMS for the decay $pp \to \tilde{b}\tilde{b}, \tilde{b} \to b\tilde{\chi}_1^0$, published in [16].

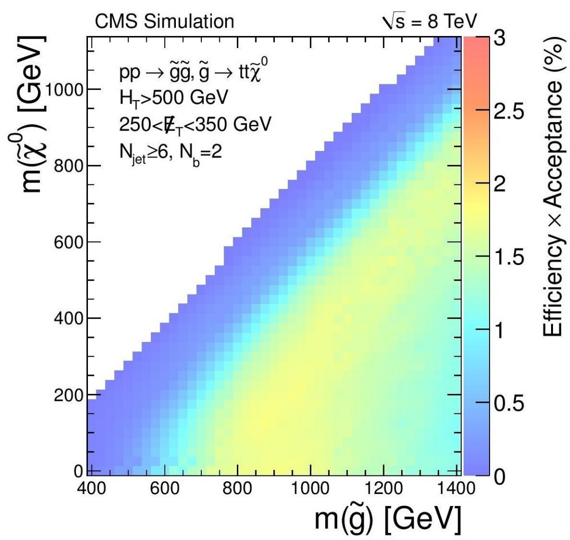

Figure 19: Efficiency map from CMS for the decay $pp \to \tilde{g}\tilde{g}, \tilde{g} \to tt\tilde{\chi}_1^0$, published in [37].

An example for an efficiency map is shown in Fig.19.

Efficiency maps are used to constrain the total signal in a specific signal region (if the correlation matrix between different signal regions is not known) which is the sum over the cross sections times branching ratios and efficiencies $\sum \sigma \times \mathcal{BR} \times \epsilon$. Here, ϵ is the efficiency which is presented in the maps as function of the masses of the new particles. It denotes the acceptance times signal efficiency $\mathcal{A} \times \epsilon$. The acceptance is determined by the geometry of the detector and the signal efficiency is determined by the analysis. It describes how many events pass the analysis cuts, for a given signal hypothesis. Therefore, each signal region corresponds to an efficiency map. The efficiency maps can be provided by the experimental groups or can also be created by phenomenologists. They can therefore also be constructed outside of the collaborations and thus provide more flexibility than upper limit maps.

Additionally to the efficiency maps, the value of the experimental upper limit on the cross section for the total signal for each signal region is provided by the experiments and stored in the `SModelS` database.

The upper limit maps constrain one simplified topology each and provide the cross section upper limit for different combinations of masses of the BSM particles appearing in the topology. The efficiency maps on the other hand provide for each signal region the efficiencies for different mass combinations in addition to the single upper limit of the cross section of the total signal.

5.2.5 Confronting theory predictions with experimental limits

With the procedure outlined in section 5.2.3 we compute a value for the cross section for every element. The next step is then to find and group all theory elements that correspond to the same experimental result. Two different elements contributing to the same result exist for example if the result asks for a lepton. From the theory side we will get elements with electrons and with muons (taus decay too fast) which will then have to be combined in order to be comparable to the experimental result.

Additionally, the elements are grouped to be compared to the experimental results which is called clustering in the `SModelS` language. The rules for clustering elements differ for UL and EM type results. For UL type results, one also has to check for the same masses of the BSM particles for a given topology. This is the case because the experimental cross section upper limit σ_{UL} is read off the UL map by asking for the masses of the BSM states. Those elements with the same (or very similar) masses are then grouped together to a cluster. The theory cross sections are then summed up for every cluster to σ_{th}. So for an UL type result there will be a list of theory cross sections and corresponding experimental cross section upper limits.

For EM type results, the theory predictions of all elements contributing to the same signal region of an experimental result are first multiplied by the corresponding efficiency read off of the efficiency map according to the masses of the BSM particles. Next, these rescaled theory cross section are all summed up. In this case it is not necessary to group the elements according to their masses since the difference in masses has already been accounted for by the efficiencies. This then gives a value for the theoretical cross section for each signal region which is then compared to the cross section upper limit σ_{UL} for this signal region.

5.2.6 The `SModelS` output

The central part of the output of `SModelS` is a list of all the experimental results that matched to some elements that resulted from the theory input file. In this list there is an entry for every signal region for EM type results and an entry for every cluster for UL type results. For each of them the theory prediction for the cross section σ_{th} and the experimental upper limit on the cross section σ_{UL} obtained as outlined before are stated and the quotient of these values is given as

$$r = \frac{\sigma_{th}}{\sigma_{UL}}. \tag{52}$$

The largest of these r-values determines whether the input theory is excluded by SModelS or not. If for the largest r-value $r > 1$, meaning that the theory prediction is larger than the experimental cross section upper limit, the point in parameter space described by the input file can be excluded. To put it in other words, if this signal existed we would have seen it. If for the largest r-value $r < 1$, the point is still allowed. This way, SModelS provides a fast method to evaluate which points of parameter space have already been ruled out by the LHC experiments and which still leave room for new physics.

5.2.7 Missing topologies

Along with the information on constrained elements, SModelS also provides information on unconstrained elements, the so-called missing topologies. The theoretical cross sections of these elements are also calculated by SModelS and these elements are then grouped. They give an overview of areas in parameter space that have not been covered by the experiments yet and so may be of interest for future analyses. Since there can be many such missing topologies only those with the highest cross sections are given in the SModelS output. By default, ten of these topologies are listed. In addition to this general group of missing topologies SModelS gives missing elements for two more specific groups of topologies that were not matched to experimental results. Those elements with more than one intermediate particle in at least one of the branches are called long cascade decays. Elements where the two branches differ from each other are called missing topologies with asymmetric branches.

5.3 SModelS version 1.2

Since SModelS version 1.0 was published in 2014 the code has developed further and many new features were added.
Of these updates version 1.2, which was released in August 2018, was the first version that introduced results with a charged stable final state in addition to the missing energy final state results [38], [39]. Results for searches with heavy stable charged particles (HSCP) and searches with R-hadrons in the final states were included. HSCP refers to particles that are electrically charged but color neutral. R-hadrons are bound states consisting of color charged BSM particles and ordinary quarks. These BSM particles would need to have a long lifetime otherwise they would have decayed before they could form such bound states.

The extensions introduced for making SModelS capable of handling these results and calculating the theory predictions for them were limited to allowing only signatures with stable charge or color non-neutral particles. Treating other signatures of long-lived particles like displaced vertices could not be implemented this way (see section 7). All principle concepts and definitions in SModelS remained conceptually unchanged. Since the modifications were aimed at introducing only signatures of stable and charged particles in the final states, issues that arise when trying to incorporate other signatures of LLPs like displaced vertices were not addressed. Most notably, the new final state particles are assumed to have such long lifetimes that they can be assumed to be entirely stable. With this assumption the efficiency and upper limit maps can be understood in the very same way as for MET results and are only functions of the masses of the BSM particles.

In contrast, the aim of this work is to upgrade SModelS to being able to handle different kinds of signatures of long-lived particles which requires more substantial extensions of both the underlying code and the understanding of the database results. However, some features were introduced in SModelS version 1.2 that are also relevant for more general signatures beyond missing energy. The most important ones are described in this section.

5.3.1 Decomposition

The decomposition procedure had to be modified in order to decompose files with stable but non-neutral particles correctly. In files leading to MET signatures the LSP simply does not have any decays and its decay width is exactly zero. This way the decomposition process stops when this particle is reached as there are no more decays provided that could be appended to the decay chain.

On the other hand, files leading to signatures with charged particles in the final states usually contain a particle with a very small but nonzero decay width. This means it also has decays listed in the file. Following the basic principles of the decomposition, these particles would be decayed until they reached the LSP. This would lead to decay chains with the particle with very small decay width as an intermediate particle. However, in previous versions of `SModelS` such decays were not allowed as such elements would not represent the correct signatures. Files containing particles with very small decay width were not treated by the original `SModelS` version.

In order to create the correct signature instead, we need an additional case where the decomposition stops when it reaches a particle with small decay width. To have the charged particle in the final state, an additional decay to the ones listed in the file is added during the decomposition. This decay symbolizes that the particle can be stable and therefore contains no particles that it decays to. The branching ratio for the particle to be stable is calculated by the reweighting function as outlined in section 7.2. As there are no decay products in this decay the decomposition would simply not continue when this particle is reached and it would then be the final BSM particle in this decay.

5.3.2 Final states

Before version 1.2 all final states are MET and it was therefore not necessary to distinguish between different types of final states. Since we now have results with different final states an additional entry describing their nature was added in the result file that stores the upper limit or efficiency map. If none are specified it is assumed by default that they are MET. These final states specified in the result files are translated to the elements built up from the constraints in the database file. This is achieved by adding an additional label to the branch holding the description of the final state as a string label, e.g. 'HSCP', defaulting to 'MET'.

The necessity of this differentiation becomes especially clear when considering elements which would look identical in the bracket notation but are not because of different Z_2-odd final states. This is for example the case for the element [[ ], [ ]] which could origin from pair production of either two MET or two stable but charged particles or a combination of the two. If these two particles had the same masses they would be considered to be identical by `SModelS`. For this reason, in version 1.2 an additional string label is added to the branch so that the elements mentioned above would appear as [[ ] , [ ]] ('MET','MET') and [[ ], [ ]] ('longlived','longlived'). This way the elements can be uniquely identified and clearly distinguished in `SModelS`.

5.3.3 Inclusive results

Many searches investigating signatures beyond missing energy present their findings in form of inclusive results. This means that the analysis does not require a set of specific SM final states. Instead they look for very prominent signatures like a heavy stable charged particle and do not put any requirements on what SM particle should be seen in association with this decay. The searches presenting such results rely on specific signatures highly distinguishable from signatures that SM particles produce (see section 4.2) and are therefore insensitive to the remaining event activity. This also means that several decay processes can contribute to the signal. The charged and stable particle could be produced through several channels and all of the channels will contribute to the measurement as the search just requires the long-lived particle itself. Inclusive searches can however also require a specific topology. For example, a search could look for a fixed topology with an inclusive SM particle. Such a search is insensitive to the nature of the SM final state. An example for an element with inclusive particles is shown in Fig.20a. On the other hand there can be an inclusive branch meaning that there can be several decays taking place but the search is entirely insensitive to the number and nature of these potential decays. An example for an element with an inclusive branch is shown in Fig.20b.

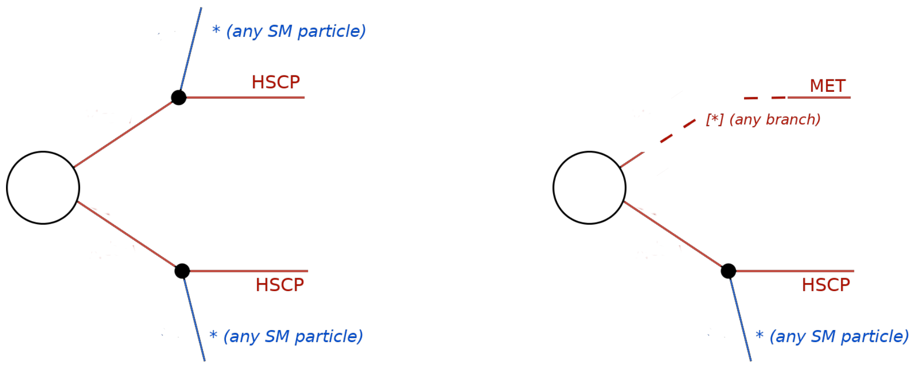

(a) Element with inclusive particles, denoted as [[['*']],[['*']]] with final states ['HSCP', 'HSCP']

(b) Element with inclusive branch, denoted as [[*],[['*']]] with final states ['MET', 'HSCP']

Figure 20: Different inclusive elements appearing in searches of the SModelS database of version 1.2, figures taken from [35].

The constraints of such searches are denoted in the SModelS database by making use of labels that represent the inclusive cases. An inclusive particle is denoted by '*' and an inclusive branch is denoted by '[*]'. These are then read in by SModelS and translated to an inclusive string or an inclusive branch object. Whenever they are compared to an object of the same type, the two objects are assigned to be equal. This allows for different elements produced during the decomposition to contribute to the theory prediction for such an inclusive results. The different decay channels contributing to an inclusive result are accounted for in this way.

5.3.4 Reweighting

In version 1.2 it is assumed that all decays happen promptly but additional to MET final states, the last particle in the decay chain can be stable and electrically or color charged (for MET it would be stable and neutral). For MET results the final Z_2-odd particle is assumed to be stable with infinite lifetime. Signatures associated with very long-lived and charged particles can also appear when it is just long-lived enough to survive the length of the detector and decays outside. These particles would also appear as stable but their cross section behaves differently than for a decay involving a truly stable particle. The number of observed events is a lifetime dependent quantity and therefore must be adjusted accordingly in SModelS. A detailed outline of the impact of finite lifetimes on the cross section, its treatment in version 1.2 with the limitations thereof and the improved handling realized in version 2.0 is given in section 7.

5.3.5 Displaced signatures in missing topologies

In the very latest release of SModelS version 1.2.2., released in November 2018 it is also possible to display elements that could lead to displaced signatures in the "missing topologies" part of the SModelS output. A displaced decay is here defined as a particle decaying outside the inner detector but within the outer detector. However, these elements do not display a full decay chain with a displaced decay in any of its intermediate decays but only gives an element up until the point where a displaced signature could arise. During the decomposition the decays are added consecutively to build up the entire decay chain. When a decay of an element has a significant fraction to result in a displaced signature, it is marked as an element with a displaced signature and the decay chain is not further built up. It is designed to list the elements that are capable of producing displaced signatures but does not give detailed information on the exact decay chains.

6 `SModelS` version 2.0 - New implementations

The upcoming update of `SModelS` which is subject of this thesis includes many changes with respect to the previous versions. These changes are mainly aimed at allowing for signatures beyond missing energy. It was therefore decided to put the entire code on a new footing and introduce a completely object oriented description of the particles. This facilitates handling the elements which are the most important structures in `SModelS`. Comparing theory predictions and experimental limits is thereby simplified. In addition, a more general restructuring of the code was carried out to improve flexibility and readability and thus make it easier to adapt for future developments. The previous releases focused on being as straightforward as possible and implement just as many features as were necessary at the time. To exemplify, for reading off the values from the experimental result maps that depend only on the masses of the BSM particles, one simply needed a unique characterization of the SM final state particles and the masses of the BSM particles. For this purpose it was enough to use strings for the SM particles and lists holding the masses. As soon as other properties are relevant it becomes cumbersome to add additional lists to store the properties. Replacing all particles by objects holding their quantum properties is the optimal solution as it allows for easy and intuitive handling of the particles and their properties. This was the starting point for the work presented here. Resulting from the introduction of particle objects many simplifications and generalizations of the code could be implemented. Also some mechanisms that are essential parts of `SModelS` as described in section 5.2 had to be rethought and restructured. Since many changes were made, an intense validation had to be carried out. To make sure the results are identical to the thoroughly validated results from previous versions the outputs were compared and differences understood.

The most relevant changes in the code are explained in greater detail in the following sections while the introduction of the lifetime dependent database results is covered in section 7.

6.1 Particle class

Originally, the elements were defined by lists of strings describing the SM particles, for example 'e-' for the electron and an array holding the masses of BSM particles appearing in the element. These two quantities together with the cross section times branching ratio of the decay then uniquely characterized an element and held all necessary information. An additional array holding the PDG numbers of the Z_2-odd particles was stored for bookkeeping only.

For signatures other than missing energy it is necessary to keep track of other particle properties like the lifetime of the particle. Other quantum numbers can also be needed like the electric charge when considering HSCP results. To simplify tracking these properties it was decided to replace the simple concept of strings and arrays with more complex class objects throughout the entire code. This allows for a more general way of treating the particles and avoids using a string label which may be user-specific.

By changing the particles from strings to objects all important structures in `SModelS` now consist of objects as well, most notably all elements with their branches. This in turn means that whenever dealing with them one now has to handle complex objects which leads to a large number of necessary adaptions. Some of these are described in detail below.

The particles now not only hold the most necessary information as before but carry all relevant properties. Even though not all of them may be used currently we provide a more general and flexible structure with this implementation allowing for easy adaption in the future. For example, one might want to take spin into account at a later point. This property is carried by the particles and currently not used but accessing it to introduce it in the calculation is straightforward now.

The properties that are stored by a particle class object are: Z_2-parity, label (a string describing the particle, e.g. 'e-'), PDG number, mass, electric charge, color charge, spin, decay width and decays to other particles. Example definitions of a SM and a BSM particle are shown in Fig.21.

```
e = Particle(            gluino = Particle(
Z2parity='even',         Z2parity='odd',
label='e-',              label='gluino',
pdg=11,                  pdg=1000021,
mass=0.5*MeV,            eCharge=0,
eCharge=-1,              colordim=8,
colordim=0,              spin=1./2)
spin=1./2,
totalwidth =
0.*GeV,
decays=[])
```

Figure 21: Example particle class definition for an electron and a gluino

The properties of the SM particles are hard-coded. The fixed properties of the BSM particles (Z_2-parity, label, PDG number, electric charge, color charge, spin) are defined in this way while their masses, decay widths and decays to other particles are read in from the input file. After these have been read in, the Z_2-odd particles have their properties updated and for every one of them the mass, decay width and decays are added as properties. This way Z_2-even and Z_2-odd particles appear in the exact same way.

6.2 Reading the input file

Before, different modules existed for reading an SLHA file and an LHE file and for their respective decomposition. In order to simplify this, the reader of the LHE files was modified so that it translates the event information to production cross sections, masses and decays as this is the information provided by SLHA files. Now the decomposition is identical for the two file formats making the specific LHE decomposer obsolete. The LHE reader goes through the file and creates dictionaries for the masses and decays of the particles. To obtain the total production cross section of a particle all cross sections of events where this particle is the mother particle are added up.

It should be noted here that the LHE decomposer assumes prompt decays of BSM particles, so this format is not suitable for meta-stable BSM particles.

6.3 Decomposition

The decomposition procedure was simplified by the LHE reader and the introduction of the particle class. The LHE reader puts the information of input LHE files into the same format as that for SLHA files and so there is only a single decomposer for both file formats. The decomposition of the file is then in principle identical to the way it was for SLHA files (see section 5.2.3). The process is however simplified as the particles now carry all the information on their masses, decay widths and decays themselves. Additional decays for stable particles other than the LSP are added in the same way as in version 1.2 which is outlined in section 5.3.1.

The production cross sections are still read directly from the file for a pair of BSM particles which are given by their PDG numbers. These numbers then get translated into the corresponding object. The full decay chain is then built up by retrieving the particle decays and corresponding branching ratios directly from the particle object which again gives particle objects holding their decays and branching ratios. The full element is built up accordingly until the LSP or a detector-stable particle is reached.

6.4 MultiParticle

Apart from the uniquely defined particles represented by instances of the particle class also more inclusive representations of particles are needed. Many experimental results are presented in terms of leptons or jets and do not and sometimes cannot differentiate between the particles contributing to each of these signatures. This used to be handled by dictionaries carrying a string describing the general particle, e.g. 'L' and the strings of their corresponding single particles, in this case ['e-','e+','mu-','mu+','tau-','tau+']. Instead of using such dictionaries we now have objects holding particle objects to represent the general particles. Therefore, the MultiParticle is introduced which carries its own identifier label (e.g. 'L' for charged lepton) and the particles belonging to this group of particles (e.g. [electron, positron, muon, anti-muon, tau, anti-tau] for charged lepton). The MultiParticle can easily be used when dealing with general particle descriptions. Furthermore, it derives from the particle class. Any property of a MultiParticle is defined as a list of that property that its individual particles have. For example the electric charge of the charged lepton MultiParticle is defined as [-1,+1] because its individual particles have either electric charge -1 or +1.

6.5 Particle types

After updating the Z_2-odd particles with the properties from the input file, all properties of all particles are defined. Depending on how the particles are used within `SModelS`, some properties are relevant while others are not needed. In order to ideally make use of the advantages of the particle objects different groups of particles are treated slightly differently. In general, elements created from the decomposition will differ from those coming from the experimental results in the way they are defined because the information available is not identical. One can roughly group the particles in three categories depending on their application.

Z_2-even Final States

These particles emerging from a vertex possess an even Z_2-parity. They are usually the SM particles but can also be Z_2-even BSM particles e.g. due to an extended Higgs sector. Which Z_2-even final state particles belong to an element is on the theory side defined by the decays in the input file and by the constraint for the search on the experiment side. These particles carry all properties as defined by the particle class.

For elements created on the experimental side there are in addition generic Z_2-even particles that are needed for inclusive results as outlined in section 5.3.3. They represent any particle that has an even Z_2-parity and is defined as

```
anyEven = Particle(label='*',Z2parity='even')
```

with the label corresponding to its representation in the database. Any particle object with even Z_2-parity is considered to be equivalent to this inclusive particle.

Z_2-odd Intermediate States

Intermediate Z_2-odd particles always decay in the form: (Z_2-odd state) $\rightarrow$ (Z_2-odd state') + Z_2-even final states. This covers all Z_2-odd particles appearing in the element and for elements produced on the theory side also includes the final stable Z_2-odd particle in the decay chain.

For elements created from the theory input in the decomposition, the intermediate states are the specific Z_2-odd particles defined in the decays. After the particles have been updated with their properties from the input file, their properties are stored differently depending on their lifetimes. In order to simplify handling the particles we distinguish between particles that decay promptly, particles that are detector-stable and particles with lifetimes in between. For this purpose we define cutoff values for the minimum decay width that a particle needs to have in order to be considered promptly decaying ('promptWidth') and a maximum decay width up to which a particle is considered stable on the detector scale ('stableWidth'). These values are by default set to $promptWidth = 10^{-8}$ GeV and $stableWidth = 10^{-25}$ GeV but can be manually set by the user in the parameter file. The chosen values provide a conservative cut for particles with very small or very large decay widths. For easy handling of the decay widths of these particles we set them to 0 GeV for those particles that are stable and to infinity for those that decay promptly. Furthermore, the spin, electric charge and color dimension of particles that are prompt are erased as these are not needed. In fact, because of these quantum numbers, `SModelS` would distinguish particles that should not be differentiated as they lead to the same detector signatures. An example for this are different types of supersymmetric partners of the quarks like the sup and sdown. In decays to SM quarks and the LSP they would both produce the exact same signature if they both decay promptly. As particles are compared by their quantum numbers, they would lead to different elements in `SModelS` because the sup and sdown have different electric charges (see also section 6.6). All particles with a decay width smaller than $promptWidth$ keep their quantum numbers.

For elements created from an experimental result, the intermediate particles are generic particles for which no properties but the Z_2-parity are specified. They are defined as

```
anyOdd = Particle(label='anyOdd',Z2parity='odd').
```

The elements on the experimental side are created from the constraints given in the result maps in the database. These constraints are given in the bracket notation (see section 5.2.2). It specifies the SM final states coming out of the decay and the topology of the associated element. This represents the result in a generic way which only depends on the masses but does not rely on the exact BSM particles involved. From the information in the constraint the element is built. The number of the generic particles for a specific element is equal to the number of vertices in the constraint and so includes all Z_2-odd particles except the stable final state.

In previous versions of `SModelS` one simply did not define any intermediate states for elements created on the experimental side.

Z_2-odd Final State Particles

The Z_2-odd particles of an element that is created on the experimental side consist of a set of generic Z_2-odd particles and in addition to that a Z_2-odd final state particle. For every final state that can currently be handled by `SModelS` (MET, HSCP, R-hadron) there exists a final state particle. The label appearing in the database entry for the experimental result describing the final state uniquely corresponds to one of these particles. Their quantum numbers are defined and correspond to the signature produced. An example for such a Z_2-odd final state particle is:

```
HSCPp = Particle(label='HSCP+', Z2parity = 'odd', eCharge = +1, colordim = 1)
```

which corresponds to a stable color neutral and positively electrically charged particle. In version 1.2 this was handled by an additional string label of the branch indicating its final state.

Making use of these newly introduced particle class objects the elements are described. The elements created from the experimental results and from the theory decomposition now appear very similarly, as can be seen in Fig.22. This facilitates the element comparison.

6.6 Element comparison

The definition of all particles as class instances provides an easier and more elegant way to keep track of the particles and their properties. It also allows for a representation of the element that

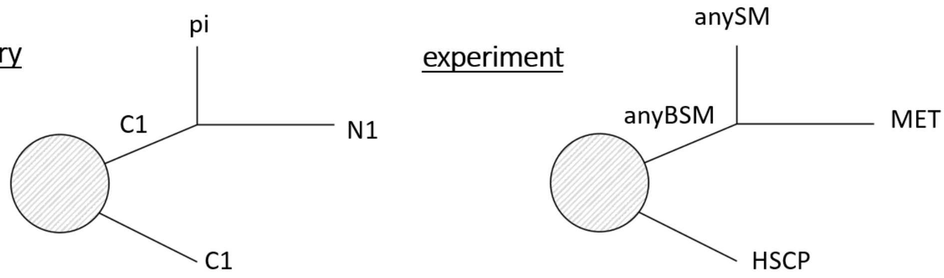

Figure 22: Two elements that would result in a match in SModelS coming from the theory decomposition procedure based on the input file and the database of experimental results.

is the same for elements constructed in the decomposition and from experimental constraints. As this was not the case before a dedicated element comparison has been developed. In previous versions the comparison of two elements from the theory side was different to the comparison of one element from the theory side to one from the experimental side. For the first case the comparison would go through the branches and determine whether the particles are the same. For the second case, the particles in the theory element first had to be replaced by their general expressions (e.g. 'l' for 'e-') and then all possible orderings of particles had to be created and determined whether either of these was identical to the particles in the constraint that one compares to. Using the modifications outlined before only a single kind of comparison is necessary now. The comparison now goes through the branches and compares the particles of the elements. As both elements from the theory and experimental side have the same structure this is straightforward.

What has become more involved is the comparison of two particles as we are now dealing with objects instead of simple strings. The equality of two strings is uniquely defined while it is more ambiguous for class instances. Therefore, a particle comparison is defined that is based on the properties. The properties that are being compared are: Z_2-parity, spin, color dimension, electric charge, mass and total decay width. As soon as one of these properties is not equal, the particles are not equal. For example, an electron is not equal to a positron because the electric charges are not equal. One can also compare a single particle to a MultiParticle which is again necessary because the particles in the experimental constraints are represented by generic labels. As for the comparison of two single particles one evaluates the properties to be compared. In the case of the MultiParticle the property is the list of this property of all particles that the MultiParticle consists of. If the particle's property is in the list of properties from the MultiParticle, they are considered equal. As an example, we consider the comparison of an electron to a charged lepton which consists of the electron, the muon, the tau and their antiparticles (see section 6.4). Their properties that are compared are:

	Z2parity	spin	colordim	eCharge	mass	totalwidth
electron	1	1/2	1	-1	0.5 MeV	0 GeV
charged lepton	[1]	[1/2]	[1]	[-1,+1]	[0.5 MeV, 106 MeV, 1777 MeV]	[0 GeV].

As all properties of the electron are in the lists of properties of the charged lepton, they are equal.

6.7 Combining elements

The produced elements are reduced to a smaller number for easier handling by combining them. In order to reduce the total number of elements that are produced and SModelS has to handle they can be combined. Whether two elements get combined is also determined by the element comparison as outlined before. If two elements are considered equal under this comparison they get combined. If the combined elements consist of particles that are identical the particles simply remain. If they differ but have the same quantum numbers used in the comparison function they are stored as a MultiParticle with the label ‘SM (combined)’ or ‘BSM (combined)’.

6.8 Element compression

The element compression reduces the steps in the decay chain which simplifies the resulting elements. It had to be changed slightly due to the introduction of long-lived particles. All elements with promptly decaying intermediate states and MET final states are compressed in the exact same way as before. For elements containing particles that are meta-stable and non-neutral as intermediate states, these decay steps should not be compressed. This can be exemplified by considering an element with a charged and long-lived particle as an intermediate state meaning that has a significantly large lifetime to be considered non-prompt but which is however short enough to allow for the particle to decay still within the detector. If this intermediate particle is close in mass to the final state particle, this step in the decay chain would be mass compressed. The original element represents a decay with a displaced signature but after compression in this way it would represent a decay with a MET signature. Therefore, these compressions should not be allowed. Fig.23 illustrates such a case. In version 1.2 these compressions were in fact carried out, while this is not the case in version 2.0. Instead, we now keep the element with the meta-stable intermediate particle as shown in the left part of the figure.

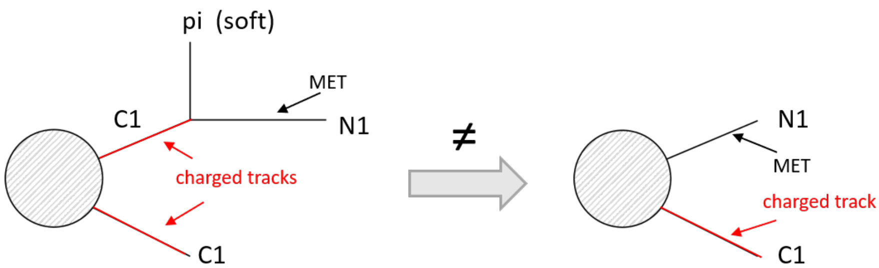

Figure 23: Example for an ‘incorrect’ mass compression where it is assumed that the chargino and neutralino are almost mass degenerate (but m(C1)>m(N1)) and the decay width of the chargino is smaller than $promptWidth$.

If the intermediate particle is however neutral and long-lived, the element should still be compressed as it still describes the correct signature. Before compressing an element we therefore check if the particle in the considered decay step is long-lived and non-neutral and do not compress if this is the case.

6.9 Element clustering

The elements are further grouped together in so-called clusters. The element clustering depends on the experimental result and is different for upper limit type results and efficiency map results. When considering general signatures of long-lived particles we also allow for a lifetime dependence in the experimental results. Details on this and how lifetime dependent maps are constructed will be outlined in section 7. For upper limit map results elements were originally clustered together if they have similar masses. When introducing lifetime this dimension also has to be added to the rules of clustering. Elements which are constrained by UL maps are therefore clustered if they have both similar masses and lifetimes. For efficiency map results all elements are always clustered together as before since the mass and lifetime dependence is already taken care of by the efficiency.

6.10 Missing topologies

Previously, the missing topologies were grouped in topologies with long cascade decays and topologies with asymmetric branches. By introducing particles with large lifetimes the grouping was replaced as the signature of a long-lived particle is a more prominent feature than either of the two previous categorizations. Instead we now group elements with at least one stable non-neutral particle, those with at least one displaced decay and all elements with promptly decaying particles and a MET final state.

6.11 Validation

The large number of changes to the code necessitated a thorough validation to confirm that the predictions that SModelS makes are still accurate. The previous versions were validated by comparing the exclusion curves given by the experiments against the exclusions computed by SModelS [34, 39]. As this has been carried out in great detail and so far no new searches were introduced, the validation for SModelS version 2.0 was done by comparing its output for $\mathcal{O}(100\text{k})$ input files against outputs for the same files produced with the previous versions of SModelS. This comparison was carried out twice. Once against the last version before version 1.2, which was version 1.1.3. This made sure that the results for MET only signatures were still as expected. It was then also compared to version 1.2 to verify that all processes relevant for particles with long lifetimes are working properly. The comparison has been carried out in several layers of accuracy in order to confirm the results as accurately as possible. The first step verifies that the same files are excluded or allowed by the two versions. Next, the highest r-value is compared. Furthermore, it is checked that there is the same number of results in the output and the r-values of all results are equal. Lastly, the cross sections of the topologies in the missing topologies and outside grid elements are compared.

Resulting from the changes introduced in version 2.0 there are inherent differences that were expected. An example is the change in the compression. A decay step in an element is in version 2.0 not compressed if the particle is long-lived and charge and color non-neutral. In version 1.2 such decay steps were compressed. Differences like this were understood in detail and the results produced by version 2.0 were thus validated.

7 Lifetime dependent results

The upper limit or efficiency maps of results for prompt searches presented by ATLAS or CMS are functions of the masses of the BSM particles appearing in the decay under consideration. Dependencies on other variables are neglected as their contribution is small. For unstable BSM particles with large lifetimes other than the lightest stable particle, the impact of finite lifetimes on the cross section or the efficiency becomes significant and cannot be neglected any longer. Correspondingly, the upper limit and efficiency maps of LLP searches do not only depend on the masses of the new particles but also on the lifetime of usually one long-lived candidate per simplified model. An example of a cross section upper limit map depending on mass and lifetime is shown in Fig.24. In this map contributions of chargino pair production $\widetilde{\chi}_1^{\pm}\widetilde{\chi}_1^{\pm}$ and production of a chargino and a neutralino $\widetilde{\chi}_1^{\pm}\widetilde{\chi}_1^{0}$ are included. It can therefore not be used by `SModelS` as only results for single simplified models can be handled and is shown here for illustration only.

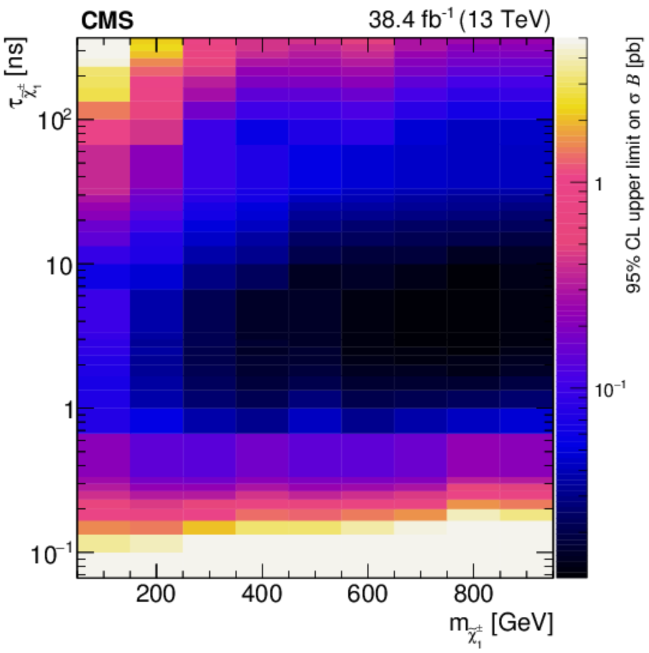

Figure 24: Cross section upper limit map for $\widetilde{\chi}_1^{\pm} \rightarrow \widetilde{\chi}_1^{0}\pi^{\pm}$ as function of mass and lifetime where it is assumed that $m(\widetilde{\chi}_1^{\pm}) \approx m(\widetilde{\chi}_1^{0})$, published in [40]

Furthermore some requirements need to be fulfilled deciding whether a search is suitable for `SModelS` or not, as in the example of Fig.24. However, we can also recreate result maps to incorporate the lifetime dependence into the efficiency or upper limit maps. This allows us to build them as functions of mass and lifetime. The principle concept of the impact of finite lifetimes on the cross section and the treatment of such results in `SModelS` will be explained. Furthermore, the calculation of lifetime dependent result maps will be outlined and an example given in this section.

7.1 Impact of finite lifetimes on the cross section

The number of events for a prompt topology ($\sigma \times \mathcal{BR}$) is given by

$$N_{events} = \mathcal{L} \times \sigma \times \mathcal{BR} \tag{53}$$

where $\mathcal{L}$ is the luminosity. The number of events changes for decays with particles with finite lifetimes. The probability for a particle decaying at time t is given by $\exp(-\frac{t}{\tau})$, where τ is the proper lifetime of the particle. The number of events corresponding to particles decaying at time t is thus given by

$$N_{events} = \mathcal{L} \times \sigma \times \mathcal{BR} \times \exp(-\frac{t}{\tau}). \tag{54}$$

We can therefore absorb the exponential factor in the cross section. Throughout this thesis, we will refer to this as lifetime dependent cross section event though in reality the total cross sections do not depend on lifetimes.

In searches for promptly decaying intermediate BSM particles and a stable neutral final state BSM particle this lifetime dependence is not relevant. The intermediate particles in MET searches have very small proper lifetimes, so the probability for them to survive even for short periods of time is very small. Its probability to decay within a very small time interval is in turn (almost) equal to 1. For the stable final state particle the situation is the exact opposite. It has infinite lifetime, so its probability to decay is 0, no matter how large the time interval. Its probability to survive on the other hand is 1. For MET results, we now need to obtain the total probability for the element to take place as all prompt decays and stable final states. We assume that the particles have lifetimes as just described above and take the product of the probabilities for the intermediate particles to decay promptly and the final state particles to survive which results in 1. Therefore, the lifetime dependence could be neglected when only considering prompt decays with MET final states.

However, as soon as one considers other signatures with long-lived particles one allows for intermediate particles with significantly large lifetimes. This in turn means that the probability for the decay of that particle within a small time interval is not necessarily close to 1, meaning it has a non-zero fraction to survive a macroscopic distance. To illustrate this Fig.25 shows the survival probabilities of particles with different decay widths $\Gamma = \frac{1}{\tau}$ as function of the distance. We call this probability $\mathcal{F}$. For a specific distance the value indicated by the curve gives the probability that the particle survives this distance while 1 minus that value gives the probability that it has decayed after this distance.

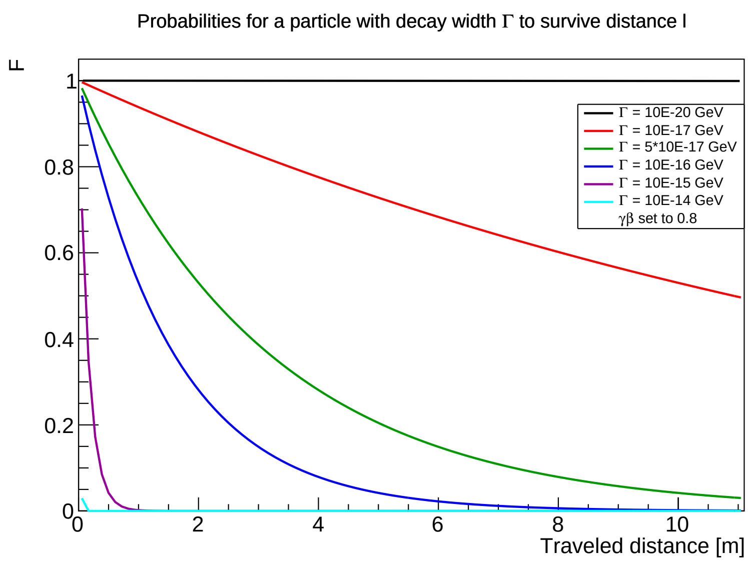

Figure 25: Probability $\mathcal{F}$ of a particle to survive a certain distance depending on its decay width Γ.

There are in principle two ways to implement these results in `SModelS`. Either the results are presented as functions of masses and lifetime and introduced in the database. In this case the lifetime dependence is an inherent feature of the result map. However, as `SModelS` was originally designed to handle maps that are exclusively functions of masses significant changes are necessary to handle such maps.

Alternatively, it is also possible to take experimental maps that are only functions of the masses and rescale the theory prediction for the cross section according to the lifetimes of the particles. To obtain the rescaled value of the cross section one needs to apply the exponential factor described before to all particles in an element. The process of rescaling the cross section is called reweighting within `SModelS`.

The second option is applied in `SModelS` version 1.2 while `SModelS` version 2.0 is also capable of directly handling lifetime dependent result maps. How this is realized in the two versions will be described in detail in the next two sections.

7.2 Reweighting in `SModelS` version 1.2

In version 1.2 only results with stable charged particles were included. These results are given as functions of the masses of the BSM particles only, in the same way as for the MET results. This is possible when assuming an infinite lifetime for the final state instead of allowing for different lifetimes of this particle. This way the map appears similarly to the MET result maps with the only difference being that the final state particle is not the LSP.

Nevertheless, there can be particles in theory that have very long lifetimes but are not entirely stable at collider scales. The newly introduced results do apply to elements with such particles as well. The theory elements with these particles as a final state are created during the decomposition as described in section 5.3.1. However, such a particle is listed in the input file like all new particles with a finite (but small) decay width and its decays with the corresponding branching ratios. For every particle, these branching ratios sum up to 1. As we now introduce an additional decay (namely that to no other particles) with some branching ratio, the total sum of all branching ratios would exceed 1. Therefore, all branching ratios including that for the case that the particle does not decay further, need to be reweighted.

For every BSM particle the probability to decay promptly which is defined as decaying within the inner detector is calculated and denoted by $\mathcal{F}_{prompt}$. In addition the probability for all BSM particles to be stable which on detector scales is defined as surviving to whole detector length is calculated and denoted by $\mathcal{F}_{long}$. The corresponding exponentials computed for every BSM particles are given by

$$\mathcal{F}_{prompt} = 1 - \exp\left(-\frac{\Gamma L_{inner}}{\langle\beta\gamma\rangle}\right) \tag{55}$$

$$\mathcal{F}_{long} = \exp\left(-\frac{\Gamma L_{outer}}{\langle\beta\gamma\rangle}\right), \tag{56}$$

where $\beta\gamma$ is the product of the velocity of the particle $\beta = \frac{v}{c}$ and the Lorentz factor $\gamma = \frac{1}{\sqrt{1-\beta^2}}$. They are set to $\langle\gamma\beta\rangle = 1.3$ when computing $\mathcal{F}_{prompt}$ and $\langle\gamma\beta\rangle = 1.43$ when computing $\mathcal{F}_{long}$. The values used for $\langle\gamma\beta\rangle$ are chosen to give conservative estimates of $\mathcal{F}_{prompt}$ and $\mathcal{F}_{long}$ as described in [39]. L_{outer} is the effective size of the whole detector (which is taken to be 10 m for both ATLAS and CMS) and L_{inner} is the effective radius of the inner detector (which is taken to be 1 mm for both ATLAS and CMS). To calculate $\mathcal{F}_{prompt}$ and $\mathcal{F}_{long}$ one also needs the decay width of the particle. As these probabilities are calculated during the decomposition where the files are being read, the decay widths of the particles can be directly obtained from the files.

The resulting rescaling factor of an element is therefore the product of the probabilities for all intermediate particles to decay promptly and the Z_2-odd final states to survive the detectors:

$$\mathcal{F}_{total} = \prod_i \mathcal{F}^i_{prompt} \times \mathcal{F}^1_{long} \times \mathcal{F}^2_{long}, \tag{57}$$

where i goes over all intermediate Z_2-odd particles and $\mathcal{F}^1_{long}$ and $\mathcal{F}^2_{long}$ belong to the two final state Z_2-odd particles. To get the correct cross section for a specific element one must therefore multiply it with this rescaling factor:

$$\sigma_{rescaled} = \sigma \times \mathcal{F}_{total}, \tag{58}$$

where sigma is defined as in section 5.2.3 as $\sigma = \sigma_{production} \times \prod_i BR_i$ and i goes over all vertices in the element. Oftentimes the lifetimes are either very large or very small resulting in $\mathcal{F}_{long} = 0$ and $\mathcal{F}_{prompt} = 1$ or the other way round. This is especially true for elements leading to MET signatures where the reweighting hardly takes an effect for most cases. However, it is now possible to constrain models with particles that have large lifetimes.

The procedure outlined above allows for successful introduction of elements with stable and charged particles in the final states. It does, however, have a few shortcomings. The $\langle \gamma\beta \rangle$ used is approximated. A particle with particularly large or small velocity could therefore receive a reweighting of its branching ratios that is very different to that calculated with its true velocity.

Furthermore, it is not straightforward to create elements with displaced vertices during the decomposition in a similar manner as for the stable charged particles. In principle one could calculate a third fraction for displaced decays and define it as

$$\mathcal{F}_{displaced} = 1 - \mathcal{F}_{prompt} - \mathcal{F}_{long}. \tag{59}$$

This would define all decays taking place outside of the inner detector but still within the whole detector as a displaced decay. However, searches looking for displaced decays distinguish between different layers of the detector where the displaced decay takes place. So displaced decays in different subdetectors are looked for by different searches. If one would group the theory elements with displaced decays defined by Eq.59 all together and match them to any displaced result, the theoretically predicted cross section would not be computed correctly. Additionally, one would have to create elements with the same topologies and particles but different intermediate decay, prompt or displaced, which would increase the total number of elements that SModelS has to handle. Fig.26 shows all elements that would be created in this case compared to the element that existed in the originally released SModelS which also did not include stable charged particles.

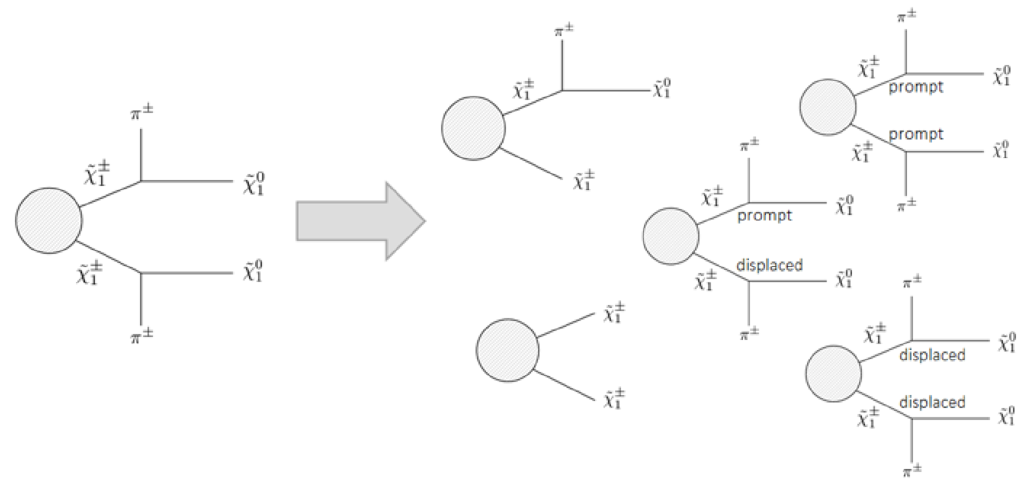

Figure 26: The element that only contains prompt decays and MET final states as it was realized in the original release of SModelS (left-hand side) and the elements with all possible combinations of decays (prompt or displaced) and final states (MET or stable and charged).

It should be noted here that in no version of SModelS, past or current, are all these elements actually created. While only the single element on the left-hand side existed in the original release, only the elements with all prompt decays and charged stable final states (in the example the two elements with charginos in the final states) were added in SModelS version 1.2. How the elements with displaced vertices are treated in SModelS version 2.0 will be outlined below.

In version 1.2 elements with displaced decays are created during the decomposition to be displayed as missing topologies. They are reweighted exactly according to Eq.59 but creating large numbers of elements is avoided by stopping the decay chain as soon as a particle with a lifetime leading to a significant probability to decay displaced is reached (see also section 5.3.5).

Furthermore, results of searches with long-lived particles are oftentimes presented as maps of masses and lifetimes. In order to read off the value of such a map for a theory element one therefore additionally needs to store the lifetimes of the particles in the elements. Of course this could principally be realized by adding an additional array holding the lifetimes of all particles appearing in the element in the same way as it has been done for the masses. Nevertheless, it was decided not to continue this way and instead opt for the introduction of a class.

7.3 Reweighting in `SModelS` version 2.0

The limitations of the reweighting of version 1.2 were crucial motivations for the introduction of the particle class and the modifications that followed from its introduction described in section 6. The reweighting procedure itself was also revised because of the approximation of the velocity of the particles and the issues arising when also displaced decays should be introduced. Furthermore, result maps that depend on masses and lifetimes are introduced which provide an improvement of the reweighting for LLP results. It also gives the possibility to implement lifetime dependent results in the database for example for searches with displaced vertices in a straightforward way.

7.3.1 Dependence on the kinematic factor

The effect that the kinematic factor $\beta\gamma$ has on the survival probability of a particle is best understood when considering the exponential function again:

$$\mathcal{F} = \exp\left(-\Gamma \times \frac{l}{\beta\gamma}\right) \tag{60}$$

with the decay width Γ, the distance l, the velocity of the particle β and the Lorentz factor γ. The effect of a variation of $\beta\gamma$ is therefore most relevant when $\Gamma l \approx 1$. l is limited by the physical dimensions of the detector with the smallest scale being the inner detector of approximately 1 mm and the largest scale the outermost layer of the detector at approximately 10 m. Consequentially, particles with intermediate lifetime that mostly decay somewhere inside the detector are most sensitive to varying $\beta\gamma$. Particles with very small decay width and so $\Gamma l \ll 1$ have a probability of about 1 to survive even the largest distance on detector scales. Particles with very large decay width and $\Gamma l \gg 1$ have a probability of about 0 to survive even the smallest distance on detector scales. $\beta\gamma$ itself is limited by the fact that BSM particles are generally expected to be heavy. Therefore, the effect of it on the survival probabilities for the two extreme groups of particles described before is marginal. Particles that decay displaced have lifetimes exactly within the range were $\beta\gamma$ becomes relevant.

The behaviour of $\beta\gamma$ was studied in order to understand its relevance. It depends on the mass of the particle since this determines how much energy is left over for the velocity of the particle after accounting for its mass. It also depends on the topology in which the particle is being produced since this also determines the distribution of the available energy. The behaviour of $\beta\gamma$ for different masses and topologies is shown Fig.27. The distributions were created with PYTHIA8 [41].

While the green, blue and red lines show the $\beta\gamma$ distribution for chargino pair production but different masses, the violet line shows the distribution for the same chargino mass as for the red line but a different topology. Especially notable is the broad spread of the distributions over a large interval of values of $\beta\gamma$ particularly for the one step decay represented by the violet line.

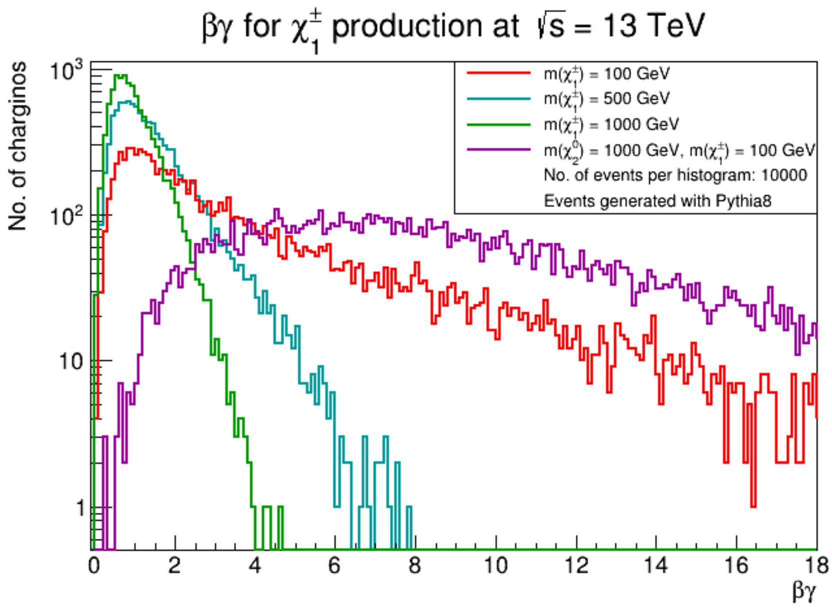

Figure 27: Distribution of $\beta\gamma$ for a stable chargino produced in chargino pair production with different masses and chargino + neutralino 2 production.

Calculating the probability of a particle to survive a certain distance with a fixed value of $\beta\gamma$ can therefore lead to unreliable values as soon as the lifetime is large enough that this factor plays a significant role. Because of this reason it was decided to revise the efficiency and cross section upper limit maps introduced in version 1.2, so the maps for decays with stable and charged particles in the final states, as for all MET results the effect is expected to be marginal. Additional to the mass dependencies a lifetime dependence of the maps is introduced. By applying the reweighting already during the construction of the maps one does not need to approximate $\beta\gamma$. With efficiency or upper limit maps that have a lifetime dependence it is no longer necessary to apply a reweighting as described in section 7.2 as this is already taken care of by the efficiencies or upper limits directly.

7.3.2 Reweighting MET results and missing topologies

As stated before, only the LLP results were modified while all MET results were kept as functions of masses only. Even though the effect is expected to be small, the efficiencies and upper limits of MET results should nevertheless be reweighted. The procedure resembles closely that of v1.2 to reweight all theory elements. An important difference now is that this reweighting is not carried out during the decomposition for all particles as we do not want to reweight elements that match to LLP results twice. Instead, the reweighting functions described in Eq.55 are applied when the value of the efficiency or cross section upper limit is read off the file for the corresponding theory element. Making use of the particle class, the masses are directly obtained from the particles and the corresponding value of the map that is only a function of the masses is read off. This value is then multiplied with the total reweighting factor for the element calculated by Eq.57 where the decay widths of the particles are also obtained directly from the particle objects.

Similarly, the cross sections of the missing topologies also have to be reweighted with the approximate functions that were also used in version 1.2. Additionally, we also want to obtain the missing topologies that include displaced decays. In version 2.0 we construct the complete decay chains which is an improvement compared to the missing topologies with displaced decays in version 1.2 which were stopped at the point where a particle that could decay displaced was encountered. For every particle in a missing topology `SModelS` now computes the probability for a prompt decay ($\mathcal{F}_{prompt}$), for a displaced decay ($\mathcal{F}_{displaced}$) and the probability for the particle to decay outside the detector ($\mathcal{F}_{long}$). We here use the same definitions as in Eq.55 and Eq.59. The definition for a displaced decay is very general since searches usually focus on displaced decays in specific sub-detectors. For the purpose of missing topologies this is nonetheless a good approximation since it covers all possibilities for displaced decays occurring for specific models. Every intermediate decay can be prompt or displaced while only the last particle can have a probability to survive the detector. This leads to several new elements arising from a single one which are constructed at this point from the element they originated from. Their weights are rescaled according to the corresponding probabilities and displayed in categories of elements with displaced decays, stable and charged final states and all prompt decays with MET final states.

7.3.3 Calculating lifetime dependent result maps

We produce result maps that are dependent on the masses and lifetimes for the results with stable charged particles in the final state that are already in the database to improve the treatment of the lifetime dependence of the cross section.

The calculation of a lifetime dependent map is outlined in the following by the example of efficiency maps constructed for a CMS HSCP search [42]. The simulations used to construct the efficiency maps are carried out with PYTHIA8 [41]. The procedure described is almost identical to the one that has been applied to create the lifetime independent maps for this search as outlined in [43]. The results thereof are in the database of SModelS version 1.2 and assume that the charged final state particles have infinite lifetime. In order to create mass and lifetime dependent maps from this search, we again apply a reweighting, only now it is already introduced during the construction of the efficiency map. This generalizes the reweighting procedure used in version 1.2 by calculating the rescaling factor per analysis and event.

We start with simulating the decays for particles with infinite lifetime and different masses of the particles. For each of these sets we then calculate values for the efficiency for several lifetimes. The procedure to obtain the efficiency for one mass and lifetime point are described for the pair production of charged and stable particles. In the simulation we produce for this case $pp \to \widetilde{\chi}_1^{\pm}\widetilde{\chi}_1^{\mp}$.

At first, the long-lived candidates are identified using truth information from the simulation. As charged stable particles show an inherently different behaviour than SM particles and are not expected to appear in close vicinity to them, the following isolation criteria are applied:

$$\sum_{charged\,particles}^{\Delta R<0.3} p_T^i < 50 \qquad\qquad \sum_{visible\,particles}^{\Delta R<0.3} \frac{p^i}{E^i} < 0.3 \tag{61}$$

where $\Delta R = \sqrt{(\Delta\eta)^2 + (\Delta\Phi)^2}$ determines the size of the cone around the direction of the long-lived candidate. Here, η is the pseudorapidity which is related to the angle of the particle relative to the beam axis, p_T is the momentum of the particle transverse to the beam direction and E is its energy. In both sums the long-lived candidate itself is not included. Muons are not considered visible particles in the sums as they release very little energy in the calorimeters. Only particles passing these cuts are considered as long-lived candidates.

The efficiency ϵ is then calculated by taking the product of the probability of the long-lived particle to survive the online and offline selection criteria, P_{on} and P_{off} given by the experiment, summed over all events and divided by the number of events:

$$\epsilon = \frac{1}{N}\sum_{i}^{N} P_{on}(\boldsymbol{k}_i) \times P_{off}(\boldsymbol{k}_i). \tag{62}$$

Here, $\boldsymbol{k}_i = (\eta_i, p_{\mathrm{T}i}, \beta_i)$ contains the kinetic properties of the long-lived particle with the pseudorapidity η, the transverse momentum p_T and the velocity β. The probabilities P_{on} and P_{off}

are read off from the table provided by the experimental groups with the corresponding $\boldsymbol{k}_i$ of the particles in that event. If there are two long-lived candidates P_{on} and P_{off} become:

$$P_{on/off} = P^1_{on/off} + P^2_{on/off} - P^1_{on/off} \times P^2_{on/off} \tag{63}$$

and then the product of P_{on} and P_{off} is taken.

To include the lifetime dependence, the probability of the particle to be detector stable (P_{ds}) is also calculated, which is simply the exponential:

$$P_{ds} = \exp\left(-\frac{1}{\tau} \times \frac{l}{\beta\gamma}\right). \tag{64}$$

Since this search is an HSCP search the respective length l is the entire length of the detector approximated with 10 m. $\beta\gamma$ is the simulated velocity of the particle in the specific event and its dependence on the mass and on the topology are inherently included as the simulation is carried out for a single decay and for a single mass. The proper lifetime τ is manually set to a fixed value.

For a pair of stable particles directly produced the total factor will be:

$$P^{total}_{ds} = P^1_{ds} \times P^2_{ds}. \tag{65}$$

The overall efficiency for a single event is then:

$$P_i = P_{on,i} \times P_{off,i} \times P^{total}_{ds,i}. \tag{66}$$

The overall efficiency for this mass and pair production of stable charged particles is then obtained by averaging over the efficiencies

$$\epsilon = \frac{1}{N}\sum_i^N P_i. \tag{67}$$

By carrying out this procedure for several masses and decay widths we obtain a map for the efficiency which is a function of mass and lifetime. The efficiency map for the example of pair production of stable and electrically charged particles is shown in Fig.28.

This map replaces the map for pair production of charged stable particles that is in the database. Following the same procedure the maps for the other topologies are produced and replace the previous charged stable maps.

7.3.4 Visualization of the lifetime reweighting

In order to visualize the effect of reweighting with lifetime one needs to turn to other particle properties than those used to calculate the efficiency. Since properties such as the kinematic factor $\beta\gamma$ or the transverse momentum p_T do not depend on the lifetime, they should not be different for different lifetimes.

The quantity L_{xy} on the other hand does depend on lifetime. It is defined as $L_{xy} = \sqrt{x^2 + y^2}$ where x and y are the coordinates of the vertex at which the particle has decayed in the plane perpendicular to the beam direction. Particles with different lifetimes should decay in different locations in the xy-plane of the detector. Therefore, the effect of reweighting can be visualized with this property. For this purpose we simulate the process $pp \to \widetilde{\chi}^{\pm}_1\widetilde{\chi}^{\mp}_1$ with two different lifetimes of the charginos and the corresponding L_{xy} are computed. Additionally, L_{xy} is computed for the simulation with the larger lifetime and L_{xy} is multiplied with the reweighting factor according to Eq.64 for every event. The lifetime τ in the reweighting factor is the smaller of the two lifetimes that is simulated separately. As can be seen in Fig.29 the quantity L_{xy} gets reproduced well by reweighting with the exponential factor. Here, L_{xy} is presented in terms of SI units.

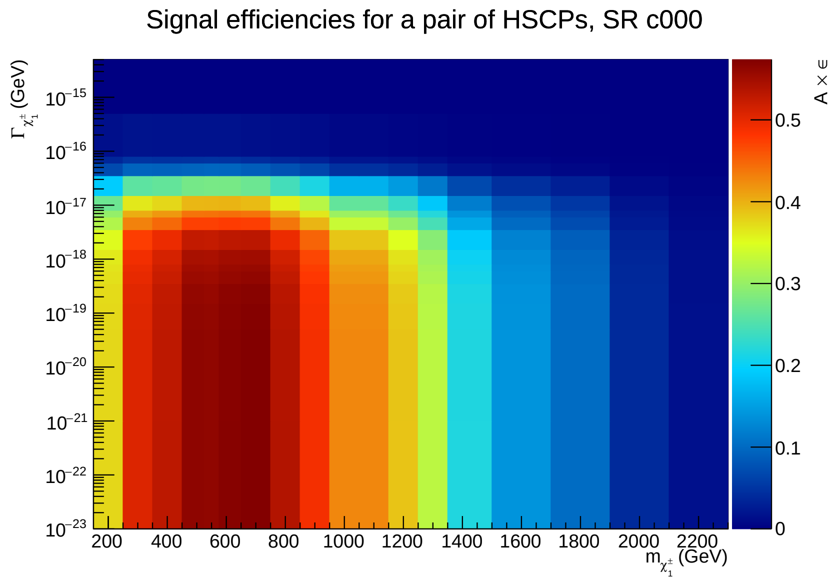

Figure 28: Mass and lifetime dependent efficiency map for pair production of stable charged particles

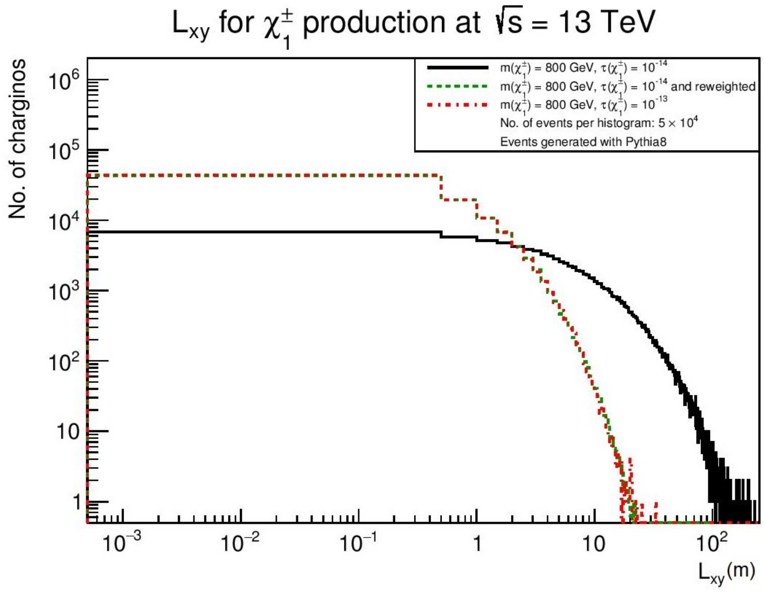

Figure 29: L_{xy} for chargino pair production with $m_{\tilde{\chi}_1^\pm} = 800$ GeV and $\tau_{\tilde{\chi}_1^\pm} = 10^{-14}$ GeV, 10^{-13} GeV. Additionally L_{xy} is shown as computed from the smaller decay width and reweighted as described for the efficiency in section 7.3.3.

7.3.5 Interpolation

When reading off the value of result maps that only depends on mass `SModelS` makes use of an sophisticated interpolation method. It is optimized for linear interpolation as the cross section and efficiency depends approximately linearly on the mass. The cross section does however depend approximately exponentially on the lifetime. So when reading off the values of a map that is a function of both mass and lifetime the interpolation implemented in `SModelS` does not give optimal results. Improvements of the interpolation are therefore necessary but lie outside the scope of this thesis.

8 Summary and Outlook

As no prominent excess in BSM searches with missing energy signatures has been detected, it has become important to systematically cover more exotic final states as well.

The open source software tool SModelS that brings together BSM theory predictions and experimental findings is therefore developed further in order to handle signatures of long-lived particles. The major modifications carried out to achieve this are presented in this thesis. The most important changes are described and the capability of the tool to apply constraints given in form of lifetime dependent maps is exemplified.

SModelS converts the information on new particles in BSM models with a Z_2-symmetry given in form of an SLHA (SUSY Les Houches Accord) or LHE (Les Houches Event) file into simplified model topologies in an automated fashion. These topologies are then compared against a large number of experimental results presented in terms of simplified models which are stored in the SModelS database. The full theory can then be constrained by several results and it is determined whether this theory has been excluded by experiments or not. It was originally aimed at searches with BSM particles that decay shortly after production and result in signatures with missing energy. As a first step to broaden this spectrum of results that are applied within SModelS, searches for stable charged particles in the final states were included in the previous release of SModelS in version 1.2. In order to be able to include other signatures as well SModelS is now restructured and a completely object oriented description of the particles is included. The class that now handles the particles stores their properties and therefore allows to access these easily at all points throughout the code. This is imperative when considering long-lived particles as one needs to be able to retrieve the particles' lifetimes but also their quantum numbers like electric or color charge in a straightforward way. Following the introduction of the particle class many modifications were carried out, including same representations of the decay chains computed from the theory input and those constructed from the constraints in the experimental results. SModelS also presents the theory predictions of decay chains that are not constrained by experiments which now also include predictions for topologies containing displaced decays. Most significantly, we have simplified the processes carried out by the tool and introduced more flexible structures. For future developments these alterations facilitate introducing new conditions defined by particle properties in the future.

Furthermore, upper limit and efficiency maps as functions of mass and lifetime can now be introduced into the database. The maps including charged stable particles in the final states were originally maps of mass only and were structurally identical to the results with MET final states. The lifetime dependence of the cross section and efficiency were handled by the so-called reweighting where the cross section is rescaled according to the survival probabilities of the particles. These maps are replaced by maps that are functions of lifetime and mass which provides a more accurate treatment of the lifetime dependence of the cross section and efficiency. It also enables SModelS to apply result maps that are presented as functions of both mass and lifetime for constraining theories. As many searches for long-lived particles present their results in this way, it is now possible to include new results into the database that could not be handled by SModelS before.

The modifications described here are crucial steps for handling more general signatures of long-lived particles and provide more flexibility for future developments. However, a few optimizations are still necessary in order to finalize SModelS version 2.0. As a logical consequence of the possibility of using mass and lifetime dependent maps in the database, a new search that provides its results in this form should be implemented into the database. An example for such a search would be a search that looks for displaced vertices. This would allow the tool to constrain theory elements that could not be constrained in any previous versions of `SModelS`. In addition, the interpolation that is used to obtain the values from mass and lifetime dependent maps is not yet optimal. It uses the same principal interpolation that was used by `SModelS` before to interpolate in maps that are only mass dependent. As this dependency is approximately linear while the dependency on lifetime is approximately exponential, this interpolation is not optimal. Both of these aspects that still require improvement do not lie within the scope of this thesis and will be left for future development.

Acknowledgements

First, I would like to thank Suchita Kulkarni for supervising this project and introducing me to the world of physics software. I always enjoyed our many interesting discussions on `SModelS`, supersymmetry and beyond. I would also like to thank Wolfgang Waltenberger for officially supervising my thesis and always being there to help when machine related problems arose. Furthermore, I want to thank Andre Lessa for all his support. Without his time and advice this work would not have been possible. I am very grateful for all improvements he suggested and helped to realize as this significantly enhanced the quality of the result of this project.
I also want to thank all members of HEPHY Apostelgasse for many entertaining discussions.
Additionally, I want to express my gratitude for the financial support by the FEMtech initiative of the BMVIT of Austria.
Finally, I want to thank my family for always supporting me.

References

[1] **ATLAS** Collaboration, G. Aad *et al.*, "Observation of a new particle in the search for the Standard Model Higgs boson with the ATLAS detector at the LHC," *Phys. Lett.* **B716** (2012) 1–29, arXiv:1207.7214 [hep-ex].

[2] **CMS** Collaboration, S. Chatrchyan *et al.*, "Observation of a new boson at a mass of 125 GeV with the CMS experiment at the LHC," *Phys. Lett.* **B716** (2012) 30–61, arXiv:1207.7235 [hep-ex].

[3] D. H. Perkins, "Introduction to high energy physics,". Cambridge University Press.

[4] G. Altarelli, "The Standard model of particle physics," arXiv:hep-ph/0510281 [hep-ph]. CERN-PH-TH-2005-206.

[5] A. Pich, "The Standard model of electroweak interactions," in *The Standard model of electroweak interactions*, pp. 1–49. 2008. arXiv:0705.4264 [hep-ph]. http://doc.cern.ch/yellowrep/2007/2007-005/cern-2007-005.pdf. [,1(2007)].

[6] ATLAS collaboration, "Atlas standard model." Https://atlas.cern/discover/physics.

[7] **Particle Data Group** Collaboration, C. Patrignani *et al.*, "Review of Particle Physics," *Chin. Phys.* **C40** no. 10, (2016) 100001.

[8] D. Hanneke, S. Fogwell, and G. Gabrielse, "New measurement of the electron magnetic moment and the fine structure constant," *Physical Review Letters* **100** no. 12, (2008) 120801.

[9] R. P. Feynman, "Space - time approach to quantum electrodynamics," *Phys. Rev.* **76** (1949) 769–789. [,99(1949)].

[10] J. Ellis, "TikZ-Feynman: Feynman diagrams with TikZ," *Comput. Phys. Commun.* **210** (2017) 103–123, arXiv:1601.05437 [hep-ph].

[11] S. Weinberg, "A Model of Leptons," *Phys. Rev. Lett.* **19** (1967) 1264–1266.

[12] A. Salam, "Weak and Electromagnetic Interactions," *Conf. Proc.* **C680519** (1968) 367–377.

[13] S. L. Glashow, "Partial Symmetries of Weak Interactions," *Nucl. Phys.* **22** (1961) 579–588.

[14] N. Cabibbo, "Unitary Symmetry and Leptonic Decays," *Phys. Rev. Lett.* **10** (1963) 531–533. [,648(1963)].

[15] M. Kobayashi and T. Maskawa, "CP Violation in the Renormalizable Theory of Weak Interaction," *Prog. Theor. Phys.* **49** (1973) 652–657.

[16] **CMS** Collaboration, A. M. Sirunyan *et al.*, "Search for supersymmetry in multijet events with missing transverse momentum in proton-proton collisions at 13 TeV," *Phys. Rev.* **D96** no. 3, (2017) 032003, arXiv:1704.07781 [hep-ex].

[17] P. W. Higgs, "Broken Symmetries and the Masses of Gauge Bosons," *Phys. Rev. Lett.* **13** (1964) 508–509. [,160(1964)].

[18] F. Englert and R. Brout, "Broken Symmetry and the Mass of Gauge Vector Mesons," *Phys. Rev. Lett.* **13** (1964) 321–323. [,157(1964)].

[19] G. 't Hooft and M. J. G. Veltman, "Regularization and Renormalization of Gauge Fields," *Nucl. Phys.* **B44** (1972) 189–213.

[20] J. Goldstone, A. Salam, and S. Weinberg, "Broken Symmetries," *Phys. Rev.* **127** (1962) 965–970.

[21] Z. Maki, M. Nakagawa, and S. Sakata, "Remarks on the unified model of elementary particles," *Prog. Theor. Phys.* **28** (1962) 870–880. [,34(1962)].

[22] B. Pontecorvo, "Neutrino Experiments and the Problem of Conservation of Leptonic Charge," *Sov. Phys. JETP* **26** (1968) 984–988. [Zh. Eksp. Teor. Fiz.53,1717(1967)].

[23] **Super-Kamiokande** Collaboration, Y. Fukuda *et al.*, "Evidence for oscillation of atmospheric neutrinos," *Phys. Rev. Lett.* **81** (1998) 1562–1567, `arXiv:hep-ex/9807003 [hep-ex]`.

[24] **SNO** Collaboration, Q. R. Ahmad *et al.*, "Direct evidence for neutrino flavor transformation from neutral current interactions in the Sudbury Neutrino Observatory," *Phys. Rev. Lett.* **89** (2002) 011301, `arXiv:nucl-ex/0204008 [nucl-ex]`.

[25] Nobel prize public information, "Running couplings." Https://www.nobelprize.org/prizes/physics/2004/popular-information/. visited on 01/15/19.

[26] C. Bambi and A. D. Dolgov, *Introduction to Particle Cosmology*. UNITEXT for Physics. Springer, 2015.

[27] R. Scarpa, "Modified Newtonian dynamics, an introductory review," *AIP Conf. Proc.* **822** (2006) 253–265, `arXiv:astro-ph/0601478 [astro-ph]`. [,253(2006)].

[28] S. P. Martin, "A Supersymmetry primer," `arXiv:hep-ph/9709356 [hep-ph]`. [Adv. Ser. Direct. High Energy Phys.18,1(1998)].

[29] **Super-Kamiokande** Collaboration, K. Abe *et al.*, "Search for proton decay via $p \to e^+\pi^0$ and $p \to \mu^+\pi^0$ in 0.31megaton $\cdot$ years exposure of the Super-Kamiokande water Cherenkov detector," *Phys. Rev.* **D95** no. 1, (2017) 012004, `arXiv:1610.03597 [hep-ex]`.

[30] L. Lee, C. Ohm, A. Soffer, and T.-T. Yu, "Collider Searches for Long-Lived Particles Beyond the Standard Model," *review* (2018) , `arXiv:1810.12602 [hep-ph]`.

[31] D. Curtin *et al.*, "Long-Lived Particles at the Energy Frontier: The MATHUSLA Physics Case," `arXiv:1806.07396 [hep-ph]`. FERMILAB-PUB-18-264-T.

[32] C. F. Kolda, "Gauge mediated supersymmetry breaking: Introduction, review and update," *Nucl. Phys. Proc. Suppl.* **62** (1998) 266–275, `arXiv:hep-ph/9707450 [hep-ph]`. [,266(1997)].

[33] C. Csaki, E. Kuflik, S. Lombardo, O. Slone, and T. Volansky, "Phenomenology of a Long-Lived LSP with R-Parity Violation," *JHEP* **08** (2015) 016, `arXiv:1505.00784 [hep-ph]`.

[34] S. Kraml, S. Kulkarni, U. Laa, A. Lessa, W. Magerl, D. Proschofsky-Spindler, and W. Waltenberger, "SModelS: a tool for interpreting simplified-model results from the LHC and its application to supersymmetry," *Eur. Phys. J.* **C74** (2014) 2868, `arXiv:1312.4175 [hep-ph]`.

[35] SModelS collaboration, "Smodels website." Https://smodels.github.io/.

[36] J. Alwall, P. Schuster, and N. Toro, "Simplified Models for a First Characterization of New Physics at the LHC," *Phys. Rev.* **D79** (2009) 075020, `arXiv:0810.3921 [hep-ph]`.

[37] **CMS** Collaboration, S. Chatrchyan *et al.*, "Search for supersymmetry in pp collisions at $\sqrt{s}$=8 TeV in events with a single lepton, large jet multiplicity, and multiple b jets," *Phys. Lett.* **B733** (2014) 328–353, `arXiv:1311.4937 [hep-ex]`.

[38] F. Ambrogi *et al.*, "SModelS v1.2: long-lived particles, combination of signal regions, and other novelties," `arXiv:1811.10624 [hep-ph]`.

[39] J. Heisig, S. Kraml, and A. Lessa, "Constraining new physics with searches for long-lived particles: Implementation into SModelS," *Phys. Lett.* **B788** (2019) 87–95, `arXiv:1808.05229 [hep-ph]`.

[40] **CMS** Collaboration, A. M. Sirunyan *et al.*, "Search for disappearing tracks as a signature of new long-lived particles in proton-proton collisions at $\sqrt{s} = 13$ TeV," *JHEP* **08** (2018) 016, `arXiv:1804.07321 [hep-ex]`.

[41] T. Sjöstrand, S. Ask, J. R. Christiansen, R. Corke, N. Desai, P. Ilten, S. Mrenna, S. Prestel, C. O. Rasmussen, and P. Z. Skands, "An Introduction to PYTHIA 8.2" *Comput. Phys. Commun.* **191** (2015) 159–177, `arXiv:1410.3012 [hep-ph]`.

[42] **CMS** Collaboration, S. Chatrchyan *et al.*, "Searches for long-lived charged particles in pp collisions at $\sqrt{s}$=7 and 8 TeV," *JHEP* **07** (2013) 122, `arXiv:1305.0491 [hep-ex]`.

[43] J. Heisig, A. Lessa, and L. Quertenmont, "Simplified Models for Exotic BSM Searches," *JHEP* **12** (2015) 087, `arXiv:1509.00473 [hep-ph]`.

List of Figures

1 Particle content of the Standard model . . . 8
2 Feynman diagram of the fundamental QED vertex . . . 11
3 Feynman diagrams of the fundamental QCD vertices . . . 13
4 Feynman diagrams of the fundamental weak vertices . . . 15
5 Feynman diagrams of the fundamental Higgs vertices . . . 17
6 QED loop correction . . . 19
7 The running gauge couplings . . . 19
8 Higgs mass loop correction . . . 20
9 Detector signatures for long-lived particles . . . 28
10 A schematic illustration of a collider detector . . . 28
11 Prompt tracks in addition to a displaced track and displaced vertices . . . 30
12 Feynman diagrams for a decay as full model and simplified model . . . 33
13 The working principles of SModelS . . . 34
14 The bracket notation in SModelS . . . 35
15 The SModelS decomposition procedure . . . 36
16 The mass compression of elements . . . 36
17 The invisible compression of elements . . . 37
18 Upper limit map example . . . 37
19 Efficiency map example . . . 37
20 Different inclusive elements appearing in searches of the SModelS database of version 1.2 . . . 41
21 Example particle class definition . . . 44
22 Matching elements in SModelS from the theory and the experimental side . . . 47
23 Incorrect mass compression . . . 48
24 Cross section upper limit map for $\widetilde{\chi}_1^{\pm} \rightarrow \widetilde{\chi}_1^0 \pi^{\pm}$ as function of mass and lifetime . 50
25 Probability of a particle to survive for different decay widths . . . 51
26 Elements with all possible combinations of decays and final states . . . 53
27 Distribution of $\beta\gamma$ for a stable chargino . . . 55
28 Mass and lifetime dependent efficiency map for pair production of stable charged particles . . . 58
29 L_{xy} for chargino pair production . . . 58

List of Tables

1 Fermions in the Standard model and their properties . . . 9
2 The chiral supermultiplets of the MSSM . . . 23
3 The vector supermultiplets of the MSSM . . . 23
4 The mass eigenstates of the MSSM . . . 24